



Hunter-gatherer sea voyages extended to remotest Mediterranean islands

Scerri, E.M.L.; Blinkhorn, J.; Groucutt, H.S.; Stewart, M.; Candy, I.; Allué, E.; ... ; Vella, N.C.

Citation

Scerri, E. M. L., Blinkhorn, J., Groucutt, H. S., Stewart, M., Candy, I., Allué, E., ... Vella, N. C. (2025). Hunter-gatherer sea voyages extended to remotest Mediterranean islands. *Nature*, 641, 137-143. doi:10.1038/s41586-025-08780-y

Version: Publisher's Version

License: [Creative Commons CC BY 4.0 license](https://creativecommons.org/licenses/by/4.0/)

Downloaded from: <https://hdl.handle.net/1887/4287766>

Note: To cite this publication please use the final published version (if applicable).

Hunter-gatherer sea voyages extended to remotest Mediterranean islands

<https://doi.org/10.1038/s41586-025-08780-y>

Received: 23 June 2024

Accepted: 12 February 2025

Published online: 9 April 2025

Open access

 Check for updates

Eleanor M. L. Scerri^{1,2,3}✉, James Blinkhorn^{1,4}✉, Huw S. Groucutt^{2,3}, Mathew Stewart⁵, Ian Candy⁶, Ethel Allué^{7,8}, Aitor Burguet-Coca^{7,8,9}, Andrés Currás¹, W. Christopher Carleton¹⁰, Susanne Lindauer¹¹, Robert Spengler¹², Ksenia Boxleitner¹², Gillian Asciak¹³, Margherita Colucci¹⁴, Ritienne Gauci¹⁵, Amy Hatton^{10,16,17}, Johanna Kutowsky¹, Andreas Maier³, Mario Mata-González¹², Nicolette Mifsud², Khady Niang^{1,18}, Patrick Roberts^{10,19}, Joshua de Giorgio²⁰, Rochelle Xerri²¹ & Nicholas C. Vella^{2,22}

The Maltese archipelago is a small island chain that is among the most remote in the Mediterranean. Humans were not thought to have reached and inhabited such small and isolated islands until the regional shift to Neolithic lifeways, around 7.5 thousand years ago (ka)¹. In the standard view, the limited resources and ecological vulnerabilities of small islands, coupled with the technological challenges of long-distance seafaring, meant that hunter-gatherers were either unable or unwilling to make these journeys^{2–4}. Here we describe chronological, archaeological, faunal and botanical data that support the presence of Holocene hunter-gatherers on the Maltese islands. At this time, Malta's geographical configuration and sea levels approximated those of the present day, necessitating seafaring distances of around 100 km from Sicily, the closest landmass. Occupations began at around 8.5 ka and are likely to have lasted until around 7.5 ka. These hunter-gatherers exploited land animals, but were also able to take advantage of marine resources and avifauna, helping to sustain these groups on a small island. Our discoveries document the longest yet-known hunter-gatherer sea crossings in the Mediterranean, raising the possibility of unknown, precocious connections across the wider region.

The emergence of long-distance seafaring varies considerably around the globe, with an early appearance in Southeast Asia and Sahul seemingly not replicated until later in other regions, such as the islands off the African coast^{5–9}. With a sea crossing of around 100 km from Sicily, and around three times as far to the Maghreb, the Maltese Archipelago is among the most remote groups of islands in the Mediterranean, the world's largest inland sea (Fig. 1). Sea-level rise rapidly submerged the low-lying, now around 95 m deep, hypothesized land bridge from Malta to Sicily around 13 ka. Over the next few thousand years, both Sicily and the Maltese islands reached their current configurations, with Malta now having a combined landmass of just 316 km² (ref. 10). Like other small Mediterranean islands, and particularly given its semi-arid climate, Malta was inferred to have been too small and remote to support human populations before the adoption of farming and more advanced seafaring technology (see Supplementary Information 1 for discussion). The general consensus has been that hunter-gatherers

only journeyed to Mediterranean islands that were large, and/or easy to reach, such as through chains of connecting islands, proximity to the mainland or favourable currents^{1,2,11} (Supplementary Information 1).

Previous research has supported this view, with the evidence suggesting that the first people to reach Malta were Neolithic farmers, associated with impressed ware pottery, stemming from the Sicilian 'Stentinello' phase of the Neolithic^{12–14}. These farmers were assumed to have introduced crops and domesticated and commensal fauna into a pristine island ecosystem¹⁴. The directly dated and secure evidence for the start of the Neolithic in Malta indicates an age of around 7.4 ka (ref. 15), which is consistent with the regional chronology of the spread of the Neolithic from southern Italy¹⁶. It is also consistent with our own chronological model (Methods, Supplementary Information 1 and Extended Data Fig. 1) based on an extensive database of radiocarbon dates with good contextual information, indicating that the earliest Neolithic in southern Italy and Sicily dates to around 7.9–7.5 ka, and

¹Human Palaeosystems Group, Max Planck Institute of Geoanthropology, Jena, Germany. ²Department of Classics and Archaeology, Faculty of Arts, University of Malta, Msida, Malta. ³Institute of Prehistoric Archaeology, University of Cologne, Cologne, Germany. ⁴Department of Archaeology, Classics and Egyptology, University of Liverpool, Liverpool, UK. ⁵Australian Research Centre for Human Evolution, Griffith University, Brisbane, Queensland, Australia. ⁶Department of Geography, Royal Holloway University of London, Egham, UK. ⁷Institut Català de Paleoecologia Humana i Evolució Social (IPHES-CERCA), Tarragona, Spain. ⁸Departament d'Història i Història de l'Art, Universitat Rovira i Virgili (URV), Tarragona, Spain. ⁹Department of Archaeological Sciences, Faculty of Archaeology, Leiden University, Leiden, The Netherlands. ¹⁰Department of Archaeology, Max Planck Institute of Geoanthropology, Jena, Germany. ¹¹Curt-Engelhorn-Centre Archaeometry, Mannheim, Germany. ¹²Domestication and Anthropogenic Evolution Research Group, Max Planck Institute of Geoanthropology, Jena, Germany. ¹³Superintendence of Cultural Heritage, Valletta, Malta. ¹⁴Evolutionary Ecology Group, Department of Zoology, University of Cambridge, Cambridge, UK. ¹⁵Department of Geography, Faculty of Arts, University of Malta, Msida, Malta. ¹⁶Department of Structural Changes of the Technosphere, Max Planck Institute of Geoanthropology, Jena, Germany. ¹⁷Institute for Archaeological Sciences, University of Tübingen, Tübingen, Germany. ¹⁸Département d'Histoire, Université Cheikh Anta Diop de Dakar, Dakar, Senegal. ¹⁹IsoTROPIC Research Group, Max Planck Institute of Geoanthropology, Jena, Germany. ²⁰Department of Archaeology, University of York, York, UK. ²¹National Museum of Natural History, Heritage Malta, Mdina, Malta. [✉]e-mail: scerri@gea.mpg.de; j.blinkhorn@liverpool.ac.uk; nicholas.vella@um.edu.mt

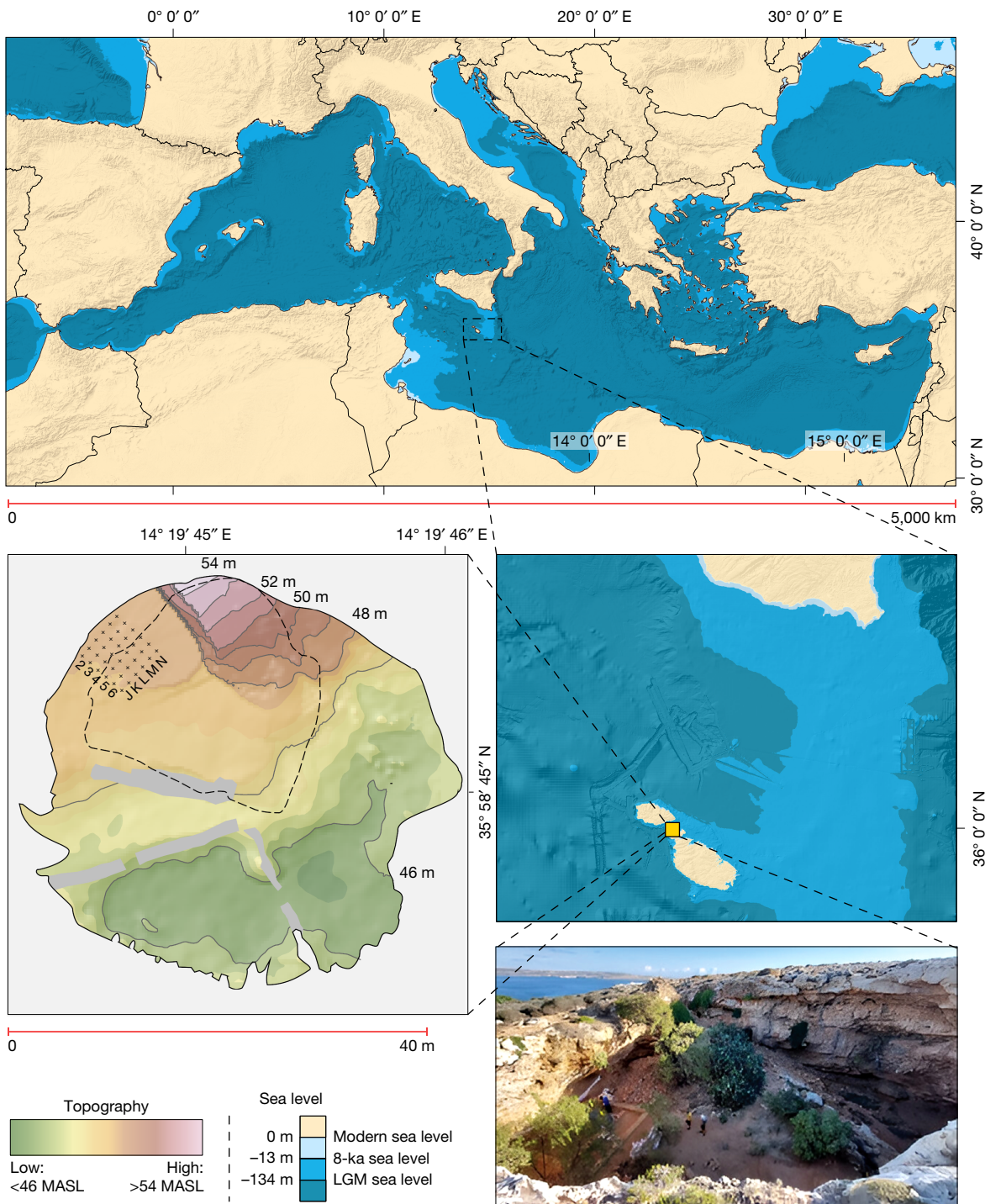


Fig. 1 | Maps and image of Latnija. Top, the position of Malta in the Mediterranean. Bottom left, digital elevation model of Latnija, showing the current dripline in dashed lines. Bottom right, the site, showing the sea channel and Gozo in the background, with past sea levels based on a previous study⁴⁹.

LGM, Last Glacial Maximum; MASL, metres above sea level. The edge of Trench 4 is denoted by the hessian sacks. Data from refs. 50,51 and created using ArcMap 10.5.

later in Malta at around 7.4–7.1 ka. Although occasional claims for an earlier Neolithic in both Sicily and Malta have been suggested, they are problematic because of radiocarbon dates and age models with high levels of uncertainty, in addition to being inconsistent with the regional chronology mentioned above (Supplementary Information 1 and Extended Data Figs. 2 and 3). Although claims of a far earlier Pleistocene human presence on Malta have also been made^{17,18}, they have so far failed to stand up to scrutiny on morphological and chronological grounds (Supplementary Information 1).

Here we provide decisive evidence for a pre-Neolithic human presence on the Maltese islands, in the form of a previously unknown Mesolithic phase characterized by the presence of Holocene hunter-gatherers. This discovery casts new light on the age and extent of Mesolithic sea crossings in the Mediterranean, and on hunter-gatherer interactions with endemic island fauna. Joint investigations led by the Max Planck Institute of Geoanthropology and the University of Malta have unravelled a deep archaeological sequence at the site of Latnija (Lat-nee-yuh). The site is located in a large doline in the Mellieħa area of northern Malta

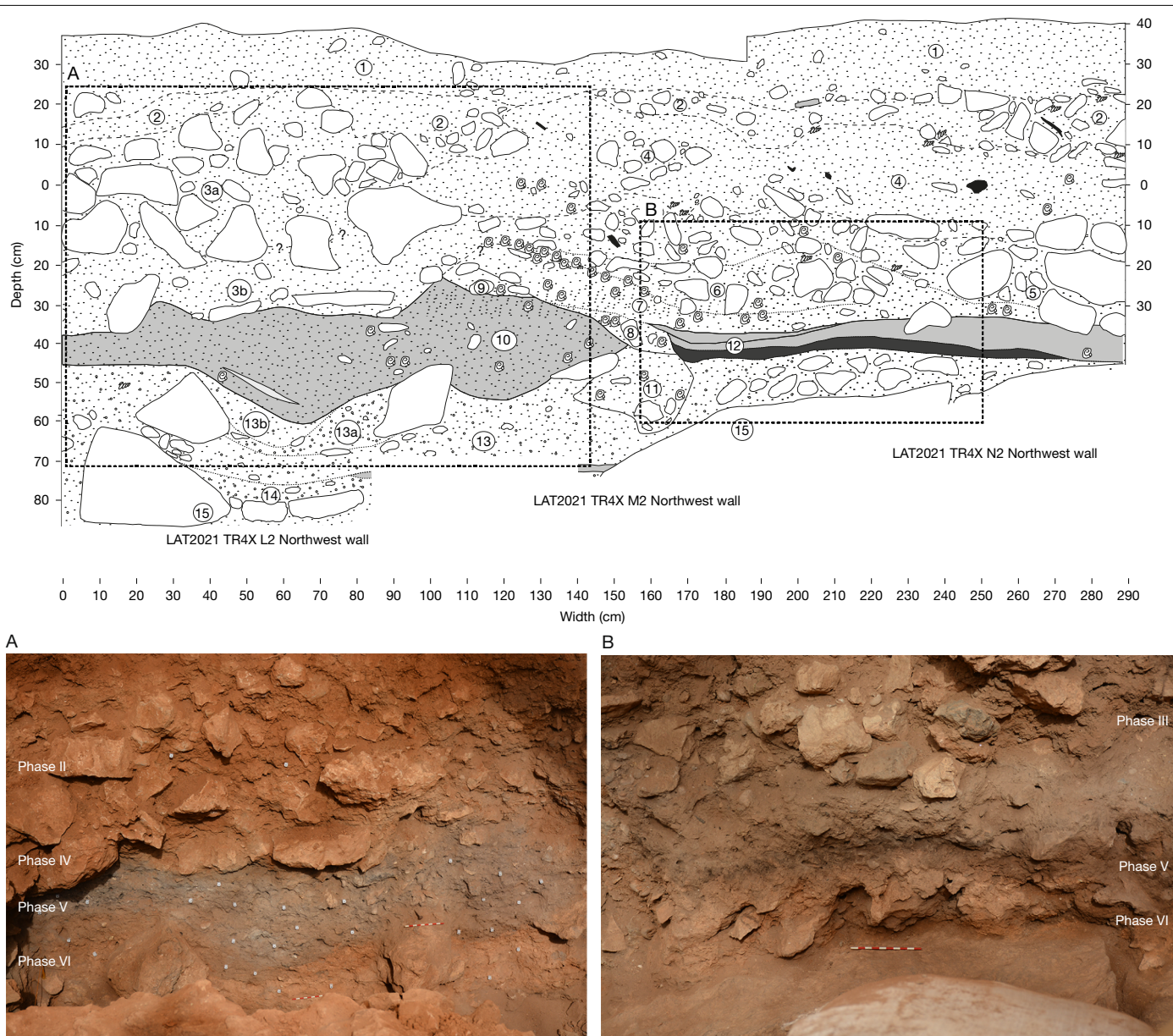


Fig. 2 | Stratigraphic section of the northwest wall. Top, illustration of the key stratigraphic sequence (numbered Beds are described in Supplementary Information 2) highlighting a thick bed of ash (A; bottom left), and a hearth deposit or combustion structure (B; bottom right), with combustion residue

(ash on top), thermal impact zone and a natural substrate (Supplementary Information 3), at the base of the Mesolithic Horizon. Note also the *Phorcus turbinatus* tip line, starting in the mid-right of box A.

(Fig. 1), in the vicinity of several fresh water sources and close to a coastline that has both sandy beaches and rocky shorelines¹⁹. Detailed excavations between 2021 and 2023 revealed early-to-mid-Holocene-aged sediments that contain stone tools, hearths, ash-tips and a range of wild flora and fauna, including marine gastropods, fish and marine mammals. These findings reveal the cultural and ecological context of the final stages of the Mesolithic, before the Neolithic transition in the region. Crucially, they also reveal the longest sea crossing yet documented in the Mediterranean by hunter-gatherers, highlighting the considerable seafaring abilities of late European hunter-gatherers. Even in the subsequent Neolithic, there are only occasional indications of such long sea crossings in the Mediterranean²⁰. Our findings upend the established notions that small and remote islands were beyond reach in the Mesolithic world.

We excavated a 5 × 5-m trench (designated Trench 4) beneath an overhang on the north-western edge of the doline, in the lee of the

prevailing northwesterly wind (Methods). We divided the trench plan into an alphanumeric grid of 1-m² squares (J–N, 2–6; Fig. 1) and recorded the position of all artefacts and bones larger than 20 mm in three dimensions using a total station. We describe the excavated sequence in six phases (labelled Phase I–VI from top to bottom), combining distinct differences in depositional processes (Supplementary Information 2) and material culture. The base of our excavated sequence (Phase VI; Fig. 2, Beds 15–13) comprises a naturally formed fine-grained cave sediment, pale orange to pink in colour (dominated by fine sands and silts), on top of sloping boulders. The character of the deposits in Phase VI is in stark contrast to that of the deposits that overlie them in Phases V–III, in which the presence of ash, fauna and shell-rich sediments presents conspicuous evidence for anthropic activity, which we refer to as the Mesolithic Horizon (Fig. 2).

The earliest Mesolithic deposit in Phase V (Fig. 2, Beds 12–10) is marked by discrete hearth features, overlain by a bed of grey ash-rich

sediment of varying thickness, a rich faunal assemblage and stone tools. The lowest hearth, from N2 (Phase V; Fig. 2 (B)), comprises two superimposed differentiated layers, as described from other sites and identified through experimental archaeology^{21,22} (Supplementary Information 2 and 3 and Fig. 2). This includes a heterogeneous light-grey ashy combustion residue of varying thickness (typically 6–12 cm) overlying a homogeneous brown-to-black thermally impacted sediment, which are distinct from the underlying Phase VI substrate (Fig. 2). Fourier transform infrared spectroscopy (FTIR) analyses confirmed that combustion residues are composed mainly of pyrogenic calcite (ash), with some thermally altered clay, which might have been introduced between burning episodes; more limited pyrogenic alteration is evident in the thermal impact zone (Supplementary Information 3). Analyses showed that higher concentrations of phytoliths were present in the same samples in which ash has been documented, compared with other parts of the combustion structure (thermal impact) and control samples (Supplementary Information 3). This indicates that the phytoliths (described below) reached the site as a result of an anthropic contribution in the form of fuel or related to use of the combustion structure. Micromorphological analysis of the sediments directly below the hearth feature in N2 show evidence for enhanced reddening and enrichment in iron oxides relative to the natural cave floor sediments (Methods and Supplementary Information 2). This is consistent with this combustion feature being in situ. In L2 and M2, micromorphology and detailed sediment analysis indicate a more complex relationship between deposits that are rich in combustion products and the sediments that underlie them; some show evidence for in situ burning, whereas others indicate erosion or cutting into the underlying sediments and the localized remobilization and redistribution of ash-rich materials (Supplementary Information 2).

The onset of episodes of cave-wall collapse is observed at the top of this ash-rich deposit, marked by a clast-dominant layer closer to the cave wall, grading to finer sediments beyond the dripline, also containing fauna and artefacts (Phase IV; Fig. 2, Bed 3b). A subcircular pit (Phase III; Fig. 2, Beds 9–5) has been dug through this layer, truncating the top of Phase V deposits; this pit contains discrete dumps of marine shells and ashes (Fig. 2 and Supplementary Information 2), as well as stone tools. The Mesolithic Horizon is sealed by more conspicuous episodes of cave-wall collapse, including both clast- and matrix-dominated cave sedimentation that contains artefacts attesting to later prehistoric, historic (Phase II; Fig. 2, Beds 4–1) and modern (Phase I) occupations.

Chronology

We selected samples for chronometric dating to constrain the age range of key sedimentary deposits, the boundaries of major sediment phases and the shells of edible marine gastropods (*Phorcus turbinatus*; $n = 49$) accumulated by humans. A total of 32 dates (obtained using accelerator mass spectrometry) on charcoal were used to constrain the different phases at the site. One additional date was also recovered on bone, whereas insufficient collagen meant that all other attempts to date bone failed (Supplementary Information 4). These dates were then calibrated to estimate the boundaries between depositional phases with a Bayesian phase model (Fig. 3, Methods and Supplementary Information 4). The results show that occupation of the site began by around 8.5 ka, well before the earliest-known dates for the arrival of Neolithic farmers in Malta and the wider region—attesting to the presence of Mesolithic hunter-gatherers. The end of the Mesolithic is more difficult to determine without precise dates for the beginning of the Neolithic at the site, but it seems to end with the arrival or establishment of the first farmers (Supplementary Information 4). The *P. turbinatus* shells were corrected for the marine reservoir effect (MRE) and calibrated ages were calculated (Methods and Supplementary Information 4). The *P. turbinatus* shells range from around 8.6 ka to 7.5 ka, supporting the charcoal age model. Crucially, the limited variability of these

shell ages supports the intact stratigraphic character of the Mesolithic Horizon, a feature particularly visible in the conspicuous tip lines in Phase III (Fig. 2 and Supplementary Information 2). Overall, the consistent chronological data and highly resolved stratigraphy support the integrity and well-dated character of the Latnija sequence.

Stone tools

A total of 64 lithics (knapped stone tools) were recovered from the Mesolithic Horizon (Phase V–III) deposits (Supplementary Information 5). Except for one chert artefact, all stone tools were made of limestone, much of which was clearly procured in the form of beach cobbles or pebbles, with the remainder sourced from terrestrial outcrops. This contrasts with younger, Neolithic, assemblages from Malta, which are made from chert (both local and imported) and small amounts of imported obsidian^{14,23,24}. Cores, blades and bladelets and retouched tools are rare in the Latnija Mesolithic assemblage, which is instead focused on simple flakes produced by hard hammer percussion. The main reduction products were squat and often cortical flakes, with generally unidirectional dorsal scar patterns. In contrast to penecontemporaneous assemblages from Sicily and other adjacent areas, which generally exhibit complex technologies and geometric forms (for example, trapezes), the lithic material from Latnija most resembles relatively expedient Mesolithic lithic technology from Sardinia²⁵ (Supplementary Information 1 and 5). The simple character of the Latnija lithic assemblage might reflect the poor quality of the limestone used and expediency, but could also reflect other factors, including demographic aspects, such as small population size and isolation.

Faunal remains

A total of 955 piece-plotted specimens (larger than 20 mm) from the Mesolithic Horizon were recorded during the 2021 and 2022 seasons, in addition to many smaller fragments recovered during sieving and flotation (Supplementary Information 6). The fauna is all wild, and overall is dominated by red deer (*Cervus elaphus*), birds and marine gastropods (*P. turbinatus* in particular, but also limpets), with the latter so far comprising some 10,000 shells (Fig. 4 and Supplementary Information 6). Small numbers of reptiles (for example, turtles and tortoises), fish (for example, groupers), crustaceans (crabs), echinoderms (sea urchins) and marine mammals (seals) were also found (Fig. 4). In line with the extensive evidence for anthropic combustion, around 25% of taphonomically studied faunal remains, including those of red deer, birds and tortoises, as well as the marine gastropods, had evidence of burning or charring (Supplementary Information 6). Although a detailed taphonomic analysis is ongoing, other traces of anthropogenic activity can also be observed, including probable percussion notches and green fracturing.

The use of marine resources, including not only small gastropods and crustaceans, but also large marine mammals, matches well with subsistence behaviours observed at other Mesolithic sites in the Mediterranean^{26–28}. Notably, studies of Neolithic and younger sites in Malta have uncovered little evidence for marine resource exploitation—and archaeological and isotopic studies suggest that people had diets that were focused mostly on terrestrial resources, including livestock and wild and domesticated plants^{15,29}. The Mesolithic deposits at Latnija therefore represent a unique level of marine resource engagement in Malta and a substantially different diet to that of later, farming communities.

Environmental reconstruction

Archaeobotanical analyses were further used to understand the environmental context of the Mesolithic Horizon. Grasses were abundant and are represented by many different phytolith morphologies

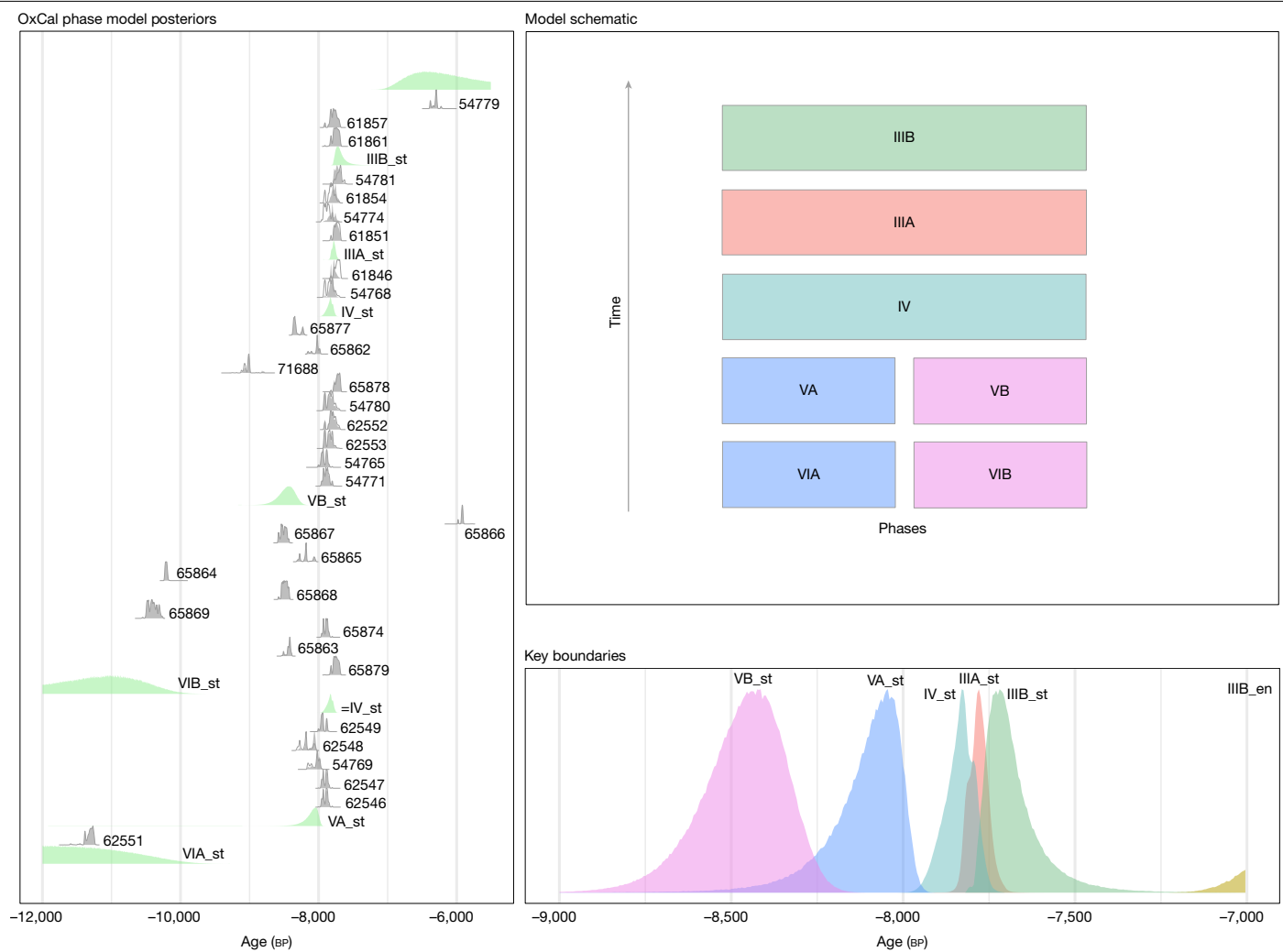


Fig. 3 | Chronological model. Model (OxCal 4.4; IntCal20) shows the phase boundaries in the Mesolithic Horizon, Phases III–V. The model indicates that the mean start date of the Mesolithic Horizon is 8.5 ka. Laboratory codes are included in the left box.

(Supplementary Information 3). Most of the grasses correspond to C_3 types, although phytolith morphologies ascribed to C_4 plants are also present. Pollen analysis of two samples from Phase V provides evidence of an open shrub vegetation consisting of *Erica multiflora* and *Euphorbia melitensis*, with patches of *Pistacia lentiscus* shrub communities occupying areas in which higher moisture levels were present and soil development occurred.

Macrobotanical samples were recovered from the systematic flotation of sediments (Methods). Seeds of a few small, wild herbaceous plants were identified, including a small-seeded grass (Poaceae), small-seeded legumes and seeds of a member of the Chenopodioideae, as well as *Mercurialis* cf. *annua* and *Vaccaria hispanica*. All of these plants grow wild on Malta today and might have been introduced to the site either by the burning of brush or through natural processes, such as the activity of rodents or birds, and inadvertently burned with cave sediments. Complementing the phytolith and macrobotanical data, the charcoal analyses reflect a shrubby vegetation adapted to the island environment, and characterized by an open scrubland dominated by *Pistacia* cf. *lentiscus*, *Juniperus* and *Tetraclinis* among other shrubs, similar to the present day. These data together indicate the presence of vegetative communities typical of the Early to Middle Holocene in the Central Mediterranean region, which have been linked to the onset of more humid climate conditions^{30–32}. These observations were further complemented by isotopic analyses of ungulate and rodent teeth from

the site (Methods and Supplementary Information 3), which indicate a fairly stable mixture of dry C_3 grassland, scrubland and woodland. In terms of plant use, the presence of the spheroid echinate phytolith morphotype in the hearth is noteworthy. This probably corresponds to the indigenous *Chamaerops humilis* (Mediterranean fan palm)³³. *Chamaerops humilis* and other palms have a wide range of uses, ranging from textiles to construction materials and food, among others. However, the greater presence of these morphotypes in the samples related to the combustion residue seems to indicate that they were also used as fuel. Anthracological analyses revealed that the most common fuel was *Pistacia* cf. *lentiscus* wood, which still grows in the vicinity of the site today. Wild seeds of grasses, and a few other low-growing herbaceous plants, were recovered in a carbonized state, either representing the burning of vegetation around the site or the construction of a hearth on top of seed-laden sediments.

Discussion

The evidence from Latnija confirms a Mesolithic occupation of the Maltese islands spanning from around 8.5 ka to 7.5 ka, which differs markedly from younger, agro-pastoral societies in technology, raw materials, diet and subsistence practices. The earliest Mesolithic arrivals on what we presume were dugout canoes, date to a time when Malta had almost reached its current configuration, which today has a

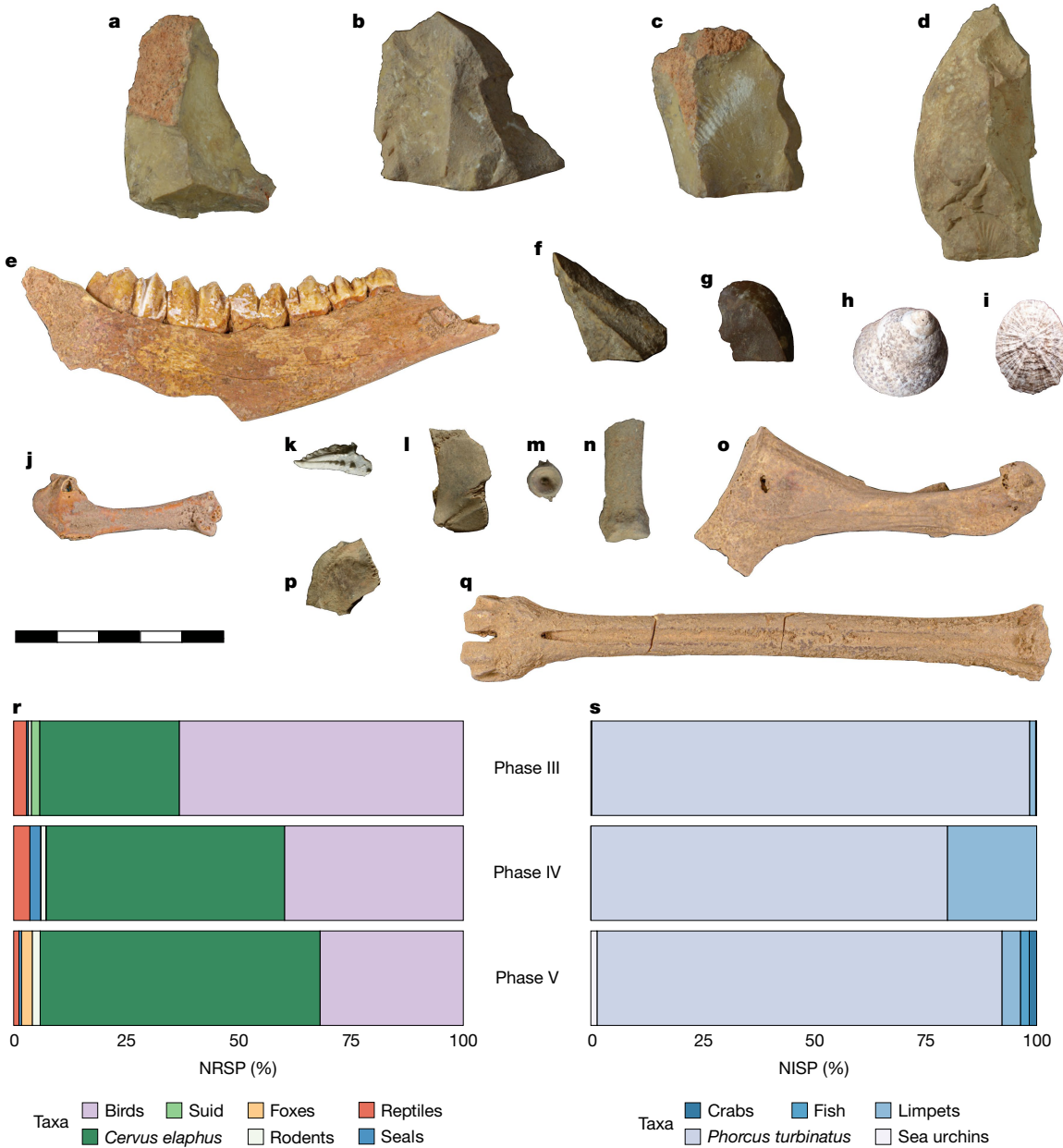


Fig. 4 | Fauna and lithics from the Mesolithic Horizon. a–q, Selected fauna and lithics from the Mesolithic Horizon. All the fauna are wild. Limestone flakes (a–d,f,g), red deer left mandible (e), and metatarsal (q), *Phorcus turbinatus* (h), *Patella* sp. (i), crab claw (k), turtle or tortoise carapace (l,p), fish vertebra (m), seal proximal phalanx (n), bird humerus (j) and coracoid (o). Scale bar is 50 mm

and applies to all. r, Percentage of the number of reported specimens (NRSP) of piece-plotted bone. This includes terrestrial animals and marine mammals. s, Percentage of the number of identified specimens (NISP) of fish and marine invertebrates from squares L2 and N2 recovered during wet sieving and flotation.

minimum straight-line distance of around 85 km to Sicily^{34,35}. However, sea surface currents and prevailing winds, as well as the use of landmarks, stars and other wayfinding practices, mean that the distances traversed by hunter-gatherers to Malta could have been considerably longer, and a crossing of about 100 km has been proposed for the Neolithic^{36–39} (Supplementary Information 1). In particular, any crossing from Sicily to Malta would have had to contend with the ocean current dynamics in the Malta Channel⁴⁰. Experimental voyages on a replica of an Early Neolithic dug-out canoe from La Marmotta (Italy) suggest that crossings of 50 km could be accomplished at a speed of about 4 km h⁻¹ (just over 2 knots)⁴¹, implying an outward summer sea journey that would have necessitated all daylight hours and an additional 8 h of darkness. In the summer, the drift caused by a southeasterly current that goes up to as much as 2 knots would have extended this outward journey even further⁴². In antiquity, as well as more historic periods,

these conditions seem to have led sailboats to prioritize ports along the Gulf of Gela as a point of departure from Sicily, rather than the closest point to Malta⁴³. These findings therefore provide evidence of long-distance, open-water sea journeys that were far longer than any previously documented in the Mediterranean, before the Neolithic and Bronze Age, when developments such as the invention of the sail occurred¹. Such inter-island crossings fall into the category of ‘difficult routes’; evidence from elsewhere suggests that canoers would avoid the dangers of voyaging at night altogether⁴⁴.

The motivation for these long sea crossings remains ambiguous. It might be that movement to Malta was driven by the availability of (perhaps seasonal) subsistence resources, catalysed by the slightly improved climate of the Early Holocene. It is also possible that the Maltese Mesolithic reflects social rather than environmental factors; namely, the potential regional demographic shockwaves through

hunter-gatherer societies associated with the transition to the Neolithic in the Mediterranean (Supplementary Information 1).

The story of Mesolithic Malta is part of a set of broader demographic and behavioural changes in the dynamic epoch of the final hunter-gatherer societies of the Mediterranean. These are both important in their own right, and also set the cultural and ecological scene for the transition to the Neolithic. The ability of Mesolithic hunter-gatherers to reach small and remote Mediterranean islands forces a re-evaluation of the capabilities and strategies of the last hunter-gatherers of the region. It also shows that Neolithic arrivals did not enter a pristine insular landscape on Malta, but rather an ecosystem that had been shaped by humans for centuries. Finally, the presence of Mesolithic hunter-gatherers on Malta raises the possibility of other long-distance connections. For example, the technological similarities between contemporary Mesolithic and Epipaleolithic communities on the African and European sides of the Mediterranean have been noted^{45–47}. The combination of several islands, and their proximity to indented mainland shorelines, has also suggested that the south-central Mediterranean and eastern Maghreb could have been a hub for early maritime activity in the region⁴⁸. The evidence we present for early long-distance seafaring from the heart of the Mediterranean adds another layer to this emerging narrative.

Online content

Any methods, additional references, Nature Portfolio reporting summaries, source data, extended data, supplementary information, acknowledgements, peer review information; details of author contributions and competing interests; and statements of data and code availability are available at <https://doi.org/10.1038/s41586-025-08780-y>.

1. Broodbank, C. *The Making of the Middle Sea: A History of the Mediterranean from the Beginning to the Emergence of the Classical World* (Thames & Hudson, 2013).
2. Broodbank, C. The origins and early development of Mediterranean maritime activity. *J. Mediterr. Archaeol.* **19**, 199–230 (2007).
3. Kelly, R. L. *The Lifeways of Hunter-Gatherers: The Foraging Spectrum* (Cambridge Univ. Press, 2013).
4. Cherry, J. F. & Leppard, T. P. Patterning and its causation in the Pre-Neolithic colonization of the Mediterranean islands (Late Pleistocene to Early Holocene). *J. Isl. Coast. Archaeol.* **13**, 191–205 (2018).
5. Clarkson, C. et al. Human occupation of northern Australia by 65,000 years ago. *Nature* **547**, 306–310 (2017).
6. Gaffney, D. Pleistocene water crossings and adaptive flexibility within the *Homo* genus. *J. Archaeol. Res.* **29**, 255–326 (2021).
7. Leppard, T. P. et al. Global patterns in island colonization during the Holocene. *J. World Prehist.* **35**, 163–232 (2022).
8. Mitchell, P. *African Islands: A Comparative Archaeology* (Routledge, 2022).
9. O'Connor, S., Kealy, S., Reepmeyer, C., Samper Carro, S. C. & Shipton, C. Terminal Pleistocene emergence of maritime interaction networks across Wallacea. *World Archaeol.* **54**, 244–263 (2022).
10. Foglini, F. et al. in *Geology and Archaeology: Submerged Landscapes of the Continental Shelf* (eds Harff, J. et al.) 77–95 (Geological Society of London, 2015).
11. Leppard, T. P. Process and dynamics of Mediterranean neolithization (7000–5500 BC). *J. Archaeol. Res.* **30**, 231–283 (2022).
12. Trump, D. H. *Skorba: Excavations Carried Out on Behalf of the National Museum of Malta, 1961–1963* (Society of Antiquaries of London, 1966).
13. Evans, J. *Prehistoric Antiquities of The Maltese Islands: A Survey* (Althone Press, 1971).
14. Malone, C. et al. *Temple Places: Excavating Cultural Sustainability in Prehistoric Malta* (McDonald Institute for Archaeological Research, 2020).
15. McLaughlin, R., Parkinson, E. W., Reimer, P. J. & Malone, C. in *Temple Places: Excavating Cultural Sustainability in Prehistoric Malta* (eds Malone, C. et al.) 27–38 (McDonald Institute for Archaeological Research, 2020).
16. Binder, D. et al. Modelling the earliest north-western dispersal of Mediterranean impressed wares: new dates and Bayesian chronological model. *Doc. Praehistor.* **44**, 54–77 (2017).
17. Keith, A. Discovery of Neanderthal man in Malta. *Nature* **101**, 404–405 (1918).
18. Mifsud, A. & Mifsud, S. *Dossier Malta—Evidence for the Magdalenian* (Proprint, 1997).
19. Environment and Resources Authority. Natura 2000 Management Planning for Terrestrial Sites in Malta and Gozo <https://era.org.mt/topic/natura-2000-management-planning-for-terrestrial-sites-in-malta-gozo> (2016).
20. Freund, K. P. & Batist, Z. Sardinian obsidian circulation and early maritime navigation in the Neolithic as shown through social network analysis. *J. Isl. Coast. Archaeol.* **9**, 364–380 (2014).
21. Mallol, C. et al. The black layer of Middle Palaeolithic combustion structures. Interpretation and archaeostratigraphic implications. *J. Archaeol. Sci.* **40**, 2515–2537 (2013).
22. Aldeias, V. Experimental approaches to archaeological fire features and their behavioral relevance. *Curr. Anthropol.* **58**, S191–S205 (2017).
23. Vella, C. Manipulated connectivity in island isolation: Maltese prehistoric stone tool technology and procurement strategies across the fourth and third millennia BC. *J. Isl. Coast. Archaeol.* **11**, 344–363 (2016).
24. Groucott, H. S. Maltese chert: an archaeological perspective on raw material and lithic technology in the central Mediterranean. *Malta Archaeol. Rev.* <https://doi.org/10.46651/mar.2022.1> (2022).
25. Lo Vetro, D. & Martini, F. Mesolithic in Central–Southern Italy: overview of lithic productions. *Quat. Int.* **423**, 279–302 (2016).
26. Mannino, M. A. et al. Climate-driven environmental changes around 8,200 years ago favoured increases in cetacean strandings and Mediterranean hunter-gatherers exploited them. *Sci. Rep.* **5**, 16288 (2015).
27. Starkovich, B. M., Munro, N. D. & Stiner, M. C. Terminal Pleistocene subsistence strategies and aquatic resource use in southern Greece. *Quat. Int.* **465**, 162–176 (2018).
28. Yu, H. et al. Genomic and dietary discontinuities during the Mesolithic and Neolithic in Sicily. *iScience* **25**, 104244 (2022).
29. McLaughlin, R. et al. in *Temple People: Bioarchaeology, Resilience and Culture in Prehistoric Malta* (eds Stoddart, S. et al.) 295–302 (McDonald Institute for Archaeological Research, 2022).
30. Tinne, W. et al. Holocene environmental and climatic changes at Gorgo Basso, a coastal lake in southern Sicily, Italy. *Quat. Sci. Rev.* **28**, 1498–1510 (2009).
31. Calò, C. et al. Spatio-temporal patterns of Holocene environmental change in southern Sicily. *Palaeogeogr. Palaeoclimatol. Palaeoecol.* **323–325**, 110–122 (2012).
32. Djalmi, M. et al. Vegetation dynamics during the early to mid-Holocene transition in NW Malta, human impact versus climatic forcing. *Veg. Hist. Archaeobot.* **22**, 367–380 (2013).
33. García-Granero, J. J. et al. A long-term assessment of the use of *Phoenix theophrasti* Greuter (Cretan Date Palm): the ethnobotany and archaeobotany of a neglected palm. *J. Ethnobiol.* **40**, 101 (2020).
34. Caruso Fermé, L., Mineo, M., Remolins, G., Mazzucco, N. & Gibaja, J. F. Navigation during the early Neolithic in the Mediterranean area: study of wooden artifacts associated with dugout canoes at La marmotta (Lago di Bracciano, Anguillara Sabazia, Lazio, Italy). *Quat. Sci. Rev.* **311**, 108129 (2023).
35. Gibaja, J. F. et al. The first Neolithic boats in the Mediterranean: the settlement of La Marmotta (Anguillara Sabazia, Lazio, Italy). *PLoS One* **19**, e0299765 (2024).
36. Irwin, G. *The Prehistoric Exploration and Colonisation of the Pacific* (Cambridge Univ. Press, 1992).
37. Bar-Yosef Mayer, D. E., Kahanov, Y., Roskin, J. & Gildor, H. Neolithic voyages to Cyprus: wind patterns, routes, and mechanisms. *J. Isl. Coast. Archaeol.* **10**, 412–435 (2015).
38. Cox, J. The orientations of prehistoric temples in Malta and Gozo. *Archaeoastronomy* **16**, 24–37 (2001).
39. Bedford, S. & Spriggs, M. *Debating Lapita: Distribution, Chronology, Society and Subsistence* (ANU Press, 2019).
40. Reyes-Suarez, N. C. et al. Sea surface circulation structures in the Malta–Sicily Channel from remote sensing data. *Water* **11**, 1589 (2019).
41. Tichy, R. The earliest maritime voyaging in the Mediterranean: view from sea. *Živá Archeologie* **18**, 26–36 (2016).
42. Heikell, R. *Mediterranean Cruising Handbook* (Imray, Laurie, Norie & Wilson, 1998).
43. Tanasi, D. & Vella, N. C. in *The Cambridge Prehistory of the Bronze and Iron Age Mediterranean* (eds Knapp, A. B. & van Dommelen, P.) 57–73 (Cambridge Univ. Press, 2015).
44. Fauvel, M. & Montenegro, A. Do stormy seas lead to better boats? Exploring the origins of the southern Californian plank canoe through ocean voyage modelling. *J. Isl. Coast. Archaeol.* **1**, 21 (2024).
45. Tixer, J. *Typologie de L'Épipaleolithique Du Maghreb* (Arts et Métiers Graphiques, 1963).
46. Laplace, G. *Recherches Sur L'Origine et L'Évolution Des Complexes Leptolithiques* (De Boccard, 1966).
47. Perrin, T. The time of the last hunters: chronocultural aspects of Early Holocene societies in the western Mediterranean. *Open Archaeol.* **9**, 20220275 (2023).
48. Broodbank, C. & Lucarini, G. The dynamics of Mediterranean Africa, ca. 9600–1000 BC. *J. Mediterr. Archaeol.* **32**, 195–267 (2019).
49. Lambeck, K., Rouby, H., Purcell, A., Sun, Y. & Cambridge, M. Sea level and global ice volumes from the Last Glacial Maximum to the Holocene. *Proc. Natl. Acad. Sci. USA* **111**, 15296–15303 (2014).
50. Japan Aerospace Exploration Agency. ALOS world 3D–30m, version 3.2 *OpenTopography* <https://doi.org/10.5069/G94M92HB> (2021).
51. GEBCO Bathymetric Compilation Group 2019. The GEBCO_2019 Grid—a continuous terrain model of the global oceans and land. *British Oceanographic Data Centre* <https://doi.org/10.5285/836f016a-33be-6ddc-e053-6c86abc0788e> (2019).

Publisher's note Springer Nature remains neutral with regard to jurisdictional claims in published maps and institutional affiliations.



Open Access This article is licensed under a Creative Commons Attribution 4.0 International License, which permits use, sharing, adaptation, distribution and reproduction in any medium or format, as long as you give appropriate credit to the original author(s) and the source, provide a link to the Creative Commons licence, and indicate if changes were made. The images or other third party material in this article are included in the article's Creative Commons licence, unless indicated otherwise in a credit line to the material. If material is not included in the article's Creative Commons licence and your intended use is not permitted by statutory regulation or exceeds the permitted use, you will need to obtain permission directly from the copyright holder. To view a copy of this licence, visit <http://creativecommons.org/licenses/by/4.0/>.

© The Author(s) 2025

Methods

Overview

Our multidisciplinary study combines archaeobotany (Supplementary Table 1), chronological modelling (Supplementary Tables 2–6), isotopes (Supplementary Table 7), contextual research and broad regional chronological modelling (Supplementary Tables 8 and 9) with anthracology and phytoliths (Supplementary Tables 10–13), lithics (Supplementary Table 14) and the study of faunal remains (Supplementary Tables 15 and 16). The methods used are described below, with further contextual information in the Supplementary Information and Extended Data Figs. 1–11.

Excavation and sedimentology

Here, we describe the excavation of a 5 × 5-m trench, designated Trench 4, at Latnija between 2021 and 2023, expanding on a 1 × 1-m test trench excavated in 2019. We set up an alphanumeric grid system in the doline to label each individual 1 × 1-m square, aligned in orientation with the 2019 test trench and with the nearby cave wall, with letters running on a SW–NE axis and numbers increasing on a NW–SE axis. The 2019 test excavation targeted square M2, with the expanded Trench 4 spanning squares J–N and 2–6, located at the northern edge of the doline spanning the dripline (Fig. 1).

Excavation was performed using a single-context recording methodology to resolve between discrete sediment units, with arbitrary subdivisions within a single deposit as 5–10-cm spits where necessary to aid control of find recovery and sediment sampling. Features of post-depositional disturbance, such as animal burrows, were readily differentiated from undisturbed sediments owing to their mixed character and friable texture and the presence of sediment voids, and were excavated in their entirety and excluded from our analyses. Finer-scale post-depositional disturbance occurs as limited fine rooting and is restricted to the uppermost deposits. The natural deposition of clasts from the shelter wall presents an alternate form of potential post-depositional disturbance that might have led to localized soft-sediment deformation. The three-dimensional position of all artefacts larger than 20 mm, bones larger than 20 mm and charcoal, and the geometry of excavation context boundaries, were recorded using a total station. Bulk sediment sampling retained a minimum of 60 l per context (predominantly in the uppermost deposits) up to 100% sampling of sediments, which were processed by bucket flotation using 250-µm mesh for macrobotanical recovery, followed by wet sieving through 5-mm screens for artefact recovery; sediments that were not retained for flotation and wet sieving were dry sieved through 5-mm screens. Additional sediment samples were recovered from each context for ancillary analyses.

So far, we have identified 309 discrete sedimentary contexts, reaching a maximum depth of 1.48 m from the surface. We have grouped contexts into six phases (Phases I to VI) on the basis of major changes in sediment colour, texture, composition and structure, alongside patterns evident in material culture. The stratigraphic matrix for the Mesolithic Horizon and immediately underlying deposits is presented in Extended Data Fig. 3.

Micromorphological samples for thin-section production were collected by cutting in situ, orientated blocks of sediment into Kubiena tins (90 mm × 70 mm × 50 mm). The location of Kubiena samples was dictated by the architecture of the sediment sequence and representative sediment deposits, and the contacts between deposits were targeted. The laboratory samples were air-dried for two weeks and placed in labelled plastic pots. The samples were immersed in a mixture of clear casting resin (four parts) to acetone (one part). To accelerate curing, a catalyst of methylethylketone peroxide was added (3 ml catalyst to 2,000 ml resin). The resin mixture was poured around the side of the sample to allow the larger pore spaces to be filled from adhesion and cohesion, and then completely immersed in the resin. The samples

were impregnated under a stepped-vacuum regime to a maximum vacuum pressure of –25 in Hg for eight hours. The samples were left to cure for around six weeks until the resin was hardened, followed by a final cure at 65 °C for 15 h. The blocks were removed from the sample frame, split along their long axes and one surface polished on fixed diamond abrasives with successively finer grades (70 µm, 45 µm and 20 µm). The polished sample was stuck to a labelled slide using an epoxy resin that cures overnight. The slide and sample were cut down to around 1 mm and then excess sample was removed using a Jones and Shipman surface grinder. The sample was hand-polished to finish off the surface before coverslipping the sample again by bonding with an epoxy resin. Analysis of the thin sections was performed on a Leica M205C petrological stereo zoom microscope and image capture was done using the Image Pro-Express software.

Archaeobotanical methods

Studies of plants in the Mesolithic Horizon at Latnija were performed in the form of pollen analyses, anthracology, hearth phytolith analyses and macrobotanical identifications from remains recovered through flotation. These analyses were performed to reconstruct the vegetation of the site, determine whether any domesticated plants were present, investigate the use of different fuels at the site and unravel mineral composition to identify combustion structures.

For pollen analysis, we collected sedimentary samples to perform palynological analyses focused on the reconstruction of past vegetation at and near Latnija. Sampling was performed in Phase V contexts (034) and (048), both of which are characterized by the presence of thick ash and combustion residue deposits. This approach was adopted to correlate the palaeobotanical remains preserved in the sediment with human activities during Phase V, which is characterized by the oldest Mesolithic.

Samples were treated following pollen concentration techniques⁵². This included sediment deflocculation with sodium pyrophosphate, Lycopodium tablets with known content to calculate palynomorph concentration values⁵³ and 7-µm nylon sieve to discard clay-sized particles. Carbonates were removed with 10% HCl and concentrated at 2,500 rpm for three minutes. Heavy liquid separation using sodium metatungstate with a specific gravity of 2.0 and centrifugation at 1,500 rpm for 20 min was done to separate organic and mineral fractions. After recovering the upper supernatant fraction, this step was repeated to increase the concentration. The remaining fraction was treated with cold 40% HF for one night to eliminate remaining silicates. The residue was washed in 98% ethanol, glycerol was added and the remaining ethanol was evaporated. The solution was kept in glycerol, mounted on slides and identified at 400× magnification under a light-transmitted microscope by referring to established literature^{54,55}. Pollen counts were done up to 250 identifiable grains. A pollen diagram (Extended Data Fig. 4a) indicating values for each taxon as percentages of the total pollen sum was plotted with the help of C2 software⁵⁶.

For anthracological analyses, bucket flotation was used to recover charcoal and other carbonized archaeobotanical remains from the sediments, all of which were collected. Charcoal was also handpicked to provide a larger number to select for dating purposes and anthracology.

A total of 165 charcoal fragments were observed under reflected light microscopy (Motic PANTHERA) with dark and bright fields and ×50, ×100, ×200 and ×500 magnifications. Images were taken with an environmental scanning electron microscope (FEI Quanta 600) coating charcoal with gold. Each charcoal piece was manually fragmented into the three wood anatomy sections (transverse, tangential and radial). Observing the three anatomy sections allowed us to identify taxonomic characters. Different wood anatomy atlases and a comparative collection at the Catalan Institute of Human Paleoenvironment and Social Evolution were used to support the identifications^{57,58}. The assemblage is characterized by a number of indeterminable fragments related to wood anatomy alterations (cracks and vitrification) and/or size of the fragments.

To study the pyroarchaeological record of the Mesolithic Horizon at Latnija, we combined the study of phytoliths and the mineralogical composition of sediments by FTIR. We analysed 24 samples that were collected during the 2022 fieldwork from a large combustion structure identified in square N2 at the base of Phase V (Fig. 2). Sampling was performed on the basis of visual identification of the internal structure of the hearth, distinguishing between samples coming from the possible combustion residue ($n = 10$), samples coming from the thermal impact zone ($n = 8$) and control samples from below the hearth ($n = 6$).

Phytoliths were extracted following the fast extraction method⁵⁹. Phytolith quantification and identification was done using a Zeiss AxioScope transmitted light microscope at $\times 200$ and $\times 400$ magnifications. Phytolith morphological identification followed the standard literature and modern plant reference collections^{33,60–62}. We followed the terminology of the International Code for Phytolith Nomenclature (ICPN 2.0) for phytolith descriptions⁶³.

The mineral composition of the samples was identified using a Jasco FT/IR-6700 spectrometer. Infrared spectra were collected in the 4,000–400 cm^{-1} wavelength range at a resolution of 4 cm^{-1} using the conventional KBr pellets method. The spectra were interpreted using the position of the main peaks described on reference collections⁶⁴. Thermally altered clay was identified on the basis of specific absorption peaks in the clay spectrum⁶⁵, and the presence of anthropogenic or geogenic calcite was determined following previous studies^{66,67}.

The archaeobotanical samples from Latnija's Mesolithic Horizon were recovered from the 2021 and 2022 excavation seasons. Although we engaged in a 100% sediment collection strategy, after flotation, not all samples from these phases contained plant macrofossils. The assemblage suitable for study consists of 28 samples in total—19 from the 2021 field season and 9 from the 2022 season. Each sample was processed in the field using a basic bucket flotation method, as described previously^{68,69}. The samples were then sent to the Max Planck Institute of Geoanthropology in Jena, Germany, for analysis. Once in the laboratory, samples were passed through nested U.S. Geological sieves to ease sorting. Material smaller than 0.50 mm was not sorted. Carbonized wood fragments larger than 2 mm were counted, although wood identification was done as a separate analysis and is reported above. Seeds and seed fragments were separated from all sieved contexts, and charred seeds were systematically collected. The identified taxa are presented in Supplementary Table 1.

Radiocarbon dating methods

Except for the bone samples, radiocarbon dating was performed at the Curt-Engelhorn-Centre Archaeometry (CEZA) in Mannheim, Germany. Samples included charcoal, seeds and marine shells. Bone samples were analysed at the University of Georgia Centre for Applied Isotope Studies (CAIS). We used a multistep chronological study to clearly constrain the Mesolithic Horizon at Latnija. First, we constructed a chronological framework for the site, which involved 31 charcoal samples and the one bone (Supplementary Tables 2 and 3). Charcoal samples were selected from contexts directly underlying the Mesolithic Horizon to help constrain the onset of Mesolithic occupation, excluding samples from burrows that appear at the interface of major divides in sediment depositional processes (Phases VI–V) (see Extended Data Fig. 5 for illustrated sample locations). In addition, charcoal samples were selected from contexts throughout the Mesolithic Horizon (Phases V–III), including direct sampling from hearths that appear at the base of Phase V (Fig. 2, Supplementary Information 2 and Extended Data Fig. 6). The model was divided into the major phases recorded during the excavation (Supplementary Information 2).

To obtain independent verification of the integrity of the age model, we also targeted marine gastropods (*P. turbinatus* in particular) because they formed clear *in situ* tip lines identified in Phase III. Forty-nine samples of *P. turbinatus* were dated for this purpose. The number of samples was chosen to reflect the fact that: (i) marine calibration is

more complex than terrestrial calibration, thus a larger sample size was required to account for the natural spread in the data; and (ii) these shells are a direct measure of human presence, because they have been imported to the site by people.

Charcoal samples were prepared using a standard ABA pretreatment. This covers an acid step with diluted hydrochloric acid to remove calcite and lime attached to the sample. A base step with diluted sodium hydroxide follows to remove soluble humic acids. As the base attracts fresh CO_2 , another acid step finalizes the pretreatment and removes any modern contamination. The samples are then combusted in an elemental analyser (MicroCube, Elementar) and the CO_2 is collected and graphitized to elemental carbon. The carbon is pressed into a target and measured in a MICADAS mass spectrometer⁷⁰.

The shell samples only undergo a treatment with diluted acid to remove adjacent carbon contamination from limestone or calcite. For shell samples, the CO_2 is extracted using phosphoric acid in an autosampler before graphitization, and measurements are the same as for the charcoal samples described in a previous study⁷¹.

The bone sample was cleaned by wire brush and washed using an ultrasonic bath. After cleaning, the sample was then reacted under vacuum with 1 M HCl to dissolve the bone mineral and release CO_2 from bioapatite. The residue was filtered, rinsed with deionized water and, under slightly acid conditions (pH 3), heated at 80 °C for six hours to dissolve collagen and leave humic substances in the precipitate. The collagen solution was then filtered to isolate pure collagen and dried out. The dried collagen was combusted at 575 °C in evacuated and sealed Pyrex ampoules in the present CuO. The resulting CO_2 was cryogenically purified from the other reaction products and catalytically converted to graphite. Graphite $^{14}\text{C}/^{13}\text{C}$ ratios were measured using the CAIS 0.5 MeV accelerator mass spectrometer. The sample ratios were compared with the ratio measured from the Oxalic Acid I (NBS SRM 4990). The uncalibrated dates were then given in radiocarbon years before 1950 (years BP), using the ^{14}C half-life of 5,568 years. The error is quoted as one standard deviation and reflects both statistical and experimental errors. The date has been corrected for isotope fractionation. As with other terrestrial radiocarbon dates in this study, calibration was performed with OxCal 4.4 using IntCal20 and as part of a phase model for the site. Modelled and unmodelled calibrated dates and model diagnostics are presented in Supplementary Tables 2 and 3.

To correct for the MRE, we compared the ages of *P. turbinatus* shells with the ages of charcoal from the same stratigraphic contexts. The reservoir effect ΔR was modelled in OxCal 4.4, with the latest datasets of IntCal20 for the charcoal samples and Marine20 for the shells. It was modelled using a phase model and choosing a wide restriction for ΔR . Samples marked by OxCal as outliers are presented in the table but are not included in the next modelling step if the model cannot deal with them leading to an A of less than 60%. These outliers might reflect processes such as bioturbation. The results of the MRE calculations are shown in Supplementary Table 4, and the corrected dates for each *P. turbinatus* age are shown in Supplementary Table 5 (see also Supplementary Information 4).

Radiocarbon modelling methods

Models involving radiocarbon dates were used to address the key question of whether there is evidence of occupation in the Latnija cave excavation sequence that securely relates to human activity predating the available evidence for Neolithic habitation elsewhere on Malta and in the surrounding Mediterranean archaeological record. This was done by: (1) establishing the age of the Mesolithic deposits at Latnija; (2) determining when the wider regional Mesolithic-to-Neolithic transition is most likely to have occurred; and (3) determining whether there is evidence for an early Neolithic occupation of Malta in a sediment core extracted from Salina Bay in northeast Malta, while accounting for the high-energy depositional environment and chronological uncertainty associated with radiocarbon dates used to produce associated

Article

age–depth models. Each of the analyses was conducted in R and is fully replicable, with scripts, data and outputs contained in a GitHub repository along with further replication instructions (<https://github.com/wccarleton/mesoneomalta>).

First, we used a standard archaeological phase model to determine start and end boundaries for major depositional phases identified at Latnija. For this model, the excavation team constructed a general Harris matrix relating different contexts to major phases of sediment deposition and artefact accumulation. Thirty-three radiocarbon samples—charcoal from short-lived local shrubs and one bone—recovered from these units were then dated and the dates were placed into an OxCal phase model to estimate phase boundary distributions. All phase boundaries were of the ‘sigma’ type. This boundary allows the tails of the distribution of events (dates) making up abutting phases to overlap. The flexibility reflects the sedimentary fuzziness inherent in the physical boundaries between depositional units. Following previously published guidance⁷², we included a general outlier model along with the phases, allowing for the model to identify potential outliers (events with extreme dates relative to both their phases and the structure of the model as a whole). The modelling identified no significant outliers among the radiocarbon-dated samples given the boundaries we used, as indicated by the posterior probabilities associated with the outlier model that indicate the probability that a given sample is an outlier in the model context (all were 8% or less; most were 4%; Supplementary Table 6).

Next, we used a cleaned regional database of radiocarbon dates associated with securely identified Mesolithic and Neolithic sites or site components from Italy, Sicily, Corsica, Sardinia and Malta. We divided the dates by region and cultural association. Then, we used a simple OxCal phase model to estimate when the Mesolithic phase ended and the Neolithic phase began in each of the regions (details in Supplementary Information 4). We used a single phase for the Mesolithic and one for the Neolithic within each region bookended by flexible ‘sigma’ boundaries, meaning that events at the end of the Mesolithic phase could occur after the estimated start-date boundary for the Neolithic. This flexibility reflects the fact that both phases refer to cultural traditions or packages that are known to have overlapped in space and time throughout the Mediterranean and that have well-established spatio-temporal trends.

Finally, we re-examined the published age–depth model for the Salina Deep sediment core. The core was argued to contain evidence for an early Neolithic in Malta, because it contains findings such as the pollen of domesticated cereals, which was estimated to date to around 8 ka on the basis of an age–depth model. However, the age–depth model used (Bchron), like many sophisticated sedimentation models, assumes monotonicity in the age–depth relationship, which we argue does not apply in the Salina Deep case. Although monotonicity is typically a good working assumption in low-energy depositional environments without evidence of disturbance, Salina Bay in the past and present is a high-energy littoral and fluvial environment that is subject to frequent storms. The core itself contains evidence of marine ingressions and many of the radiocarbon dates indicate substantial sediment redeposition, with very old dates near the surface and segments showing a wide radiocarbon temporal spread. Together, this evidence suggests that monotonicity is a poor assumption for Salina Deep and, consequently, that the published age–depth model is overly (unduly) precise because it cannot account for the wide variance in radiocarbon sample dates for many of the core’s segments. To account for this, and produce a model that is more representative of the empirical temporal variance, we used a linear Bayesian regression to model the age–depth relationship. The model recognizes a general relationship in the available age–depth observations indicating a trend toward older dates correlated with depth. However, it also does not assume strict monotonicity, instead focusing on the broad age–depth relationship. We used a custom distribution (based on standard radiocarbon-date calibration) to add

a measurement uncertainty component to the model, representing radiocarbon dating and calibration uncertainties. We also used Bayesian imputation to model dates with full posterior uncertainty for a sequence of undated sediment depths (see Supplementary Information 1 for further details).

Zooarchaeological methods

During the 2021 and 2022 field seasons, faunal remains greater than 20 mm in length were piece plotted using a total station, given a unique identifier and bagged. Smaller bone fragments, shells and other faunal remains were recovered through various methods, including an exhaustive programme of wet sieving, flotation and manual inspection of 8-mm, 4-mm, 2-mm, 1-mm and 0.5-mm sieved sinks under microscopy. Here we present a preliminary taxonomic and taphonomic analysis of this faunal material, but note that a full detailed analysis is currently underway that comprises all remains recovered during excavation.

Bones were identified to skeletal element and, for the most part, to broad taxonomic categories (for example, fish and birds), facilitated by relevant literature^{73–76}, online resources and comparative material housed at the University of Malta. The taphonomic analysis focused on identifying bone fractures and surface modifications, such as burning, butchery marks (such as cut marks) and carnivore damage (for example, gnawing) following standard protocols^{77–80}. Remains are reported as the number of specimens (NRSP) and number of identified specimens (NISP), following a previous report⁸¹. NRSP includes all skeletal remains (bones and teeth) included in this study, whereas NISP is defined as all skeletal elements (bones and teeth) identified minimally to class.

In addition to the piece-plotted bone, we also report here the complete counts of marine fauna for two excavation squares (L2 and N2), reflecting material that was directly recovered and bagged during excavation and material from wet sieving and flotation. Given the very different sediment volumes exposed for the different phases, we chose here to focus at first on these two squares, which offer a good sequence through the phases, to showcase the marine component at the site.

Isotope methods

Nineteen samples, comprising 12 wood mouse (*Apodemus sylvaticus*) and 7 red deer (*Cervus elaphus*), were selected for $\delta^{13}\text{C}$ and $\delta^{18}\text{O}$ isotope analysis of tooth enamel (Supplementary Table 7). For red deer, molar teeth were targeted for analysis, although the sample set does include one red deer premolar tooth. It should also be noted that because some of these samples are non-overlapping teeth, it is possible that some pseudo-sampling (sampling from the same individual) took place. For wood mouse, whole molar and incisor teeth were used to ensure that the minimum sample size for stable isotope analysis was met.

Before sampling, red deer were cleaned through gentle abrasion with a diamond-tipped drill to remove any adhering material. After cleaning, the same approach was used to sample the tooth enamel along the full length of the buccal surface to ensure a representative measurement for the period of tooth formation. For wood mouse, as much of the dentine was removed as possible using a drill before the remaining whole teeth were crushed using a mortar and pestle, with cleaning of the mortar and pestle using 70% ethanol between samples.

To remove organic or secondary carbonate contaminants, all samples underwent pretreatment, which involved soaking in 0.1 M acetic acid for 10 min followed by three rinses in purified water^{82,83}. After reaction with 100% phosphoric acid, gasses were analysed using a Thermo Gas-Bench II connected to a Thermo Delta V Advantage mass spectrometer housed at the Department of Archaeology at the Max Planck Institute of Geoanthropology. Carbon and oxygen isotopes are reported as the ratio of heavier to lighter isotopes ($^{13}\text{C}/^{12}\text{C}$ or $^{18}\text{O}/^{16}\text{O}$) in parts per million (‰) relative to international standards (Vienna PeeDee Belemnite, VPDB). $\delta^{13}\text{C}$ and $\delta^{18}\text{O}$ values were normalized using a three-point

calibration against the international standards IAEA-603 ($\delta^{13}\text{C} = 2.5\text{\textperthousand}$, $\delta^{18}\text{O} = -2.4\text{\textperthousand}$), IAEA-CO-8 ($\delta^{13}\text{C} = -5.8\text{\textperthousand}$, $\delta^{18}\text{O} = -22.7\text{\textperthousand}$) and IAEA NBS 18 ($\delta^{13}\text{C} = -5.014\text{\textperthousand}$, $\delta^{18}\text{O} = 23.2\text{\textperthousand}$), as well as the in-house standard of USGS44 ($\delta^{13}\text{C} = -42.2\text{\textperthousand}$).

Reporting summary

Further information on research design is available in the Nature Portfolio Reporting Summary linked to this article.

Data availability

Data required to reproduce the chronological models are available at <https://github.com/wccarleton/mesoneomalta>, and are archived with Zenodo at <https://doi.org/10.5281/zenodo.14192393> (ref. 84).

Code availability

Code required for reproducing the chronological models is available at <https://github.com/wccarleton/mesoneomalta>, and is archived with Zenodo at <https://doi.org/10.5281/zenodo.14192393> (ref. 84).

52. Florenzano, A. et al. The significance of intestinal parasite remains in pollen samples from medieval pits in the Piazza Garibaldi of Parma, Emilia Romagna, northern Italy. *Geoarchaeology* **27**, 34–47 (2012).
53. Stockmarr, J. Tablets with spores used in absolute pollen analysis. *Pollen et Spores* **13**, 615–621 (1971).
54. Reille, M. *Pollen et Spores d'Europe et d'Afrique Du Nord* (Laboratoire de Botanique Historique et Palynologie, 1999).
55. Beug, H.-J. *Leitfaden Der Pollenbestimmung Für Mitteleuropa Und Angrenzende Gebiete* (Verlag Friedrich Pfeil, 2004).
56. Juggins, S. Software for ecological and palaeoecological data analysis and visualisation. User guide, version 1.5 <http://www.campus.ncl.ac.uk/staff/Stephen.Juggins/software/C2Home.htm> (Newcastle University, 2007).
57. Wheeler, E. A. InsideWood—a web resource for hardwood identification. *IAWA J.* **32**, 199–211 (2011).
58. Schweingruber, F. H. *Anatomy of European Woods: An Atlas for the Identification of European Trees, Shrubs and Dwarf Shrubs* (Verlag Kessel, 1990).
59. Katz, O. et al. Rapid phytolith extraction for analysis of phytolith concentrations and assemblages during an excavation: an application at Tell es-Safi/Gath, Israel. *J. Archaeol. Sci.* **37**, 1557–1563 (2010).
60. Piperno, D. R. *Phytoliths: A Comprehensive Guide for Archaeologists and Paleoecologists* (AltaMira Press, 2006).
61. Rapp, G. & Mulholland, S. G. *Phytolith Systematics: Emerging Issues* (Plenum Press, 1992).
62. Twiss, P. C. in *Phytolith Systematics: Emerging Issues* (eds Rapp, G. & Mulholland, S. C.) 113–128 (Plenum Press, 1992).
63. Neumann, K. et al. International code for phytolith nomenclature (ICPN) 2.0. *Ann. Bot.* **124**, 189–199 (2019).
64. Weiner, S. *Microarchaeology Beyond the Visible Archaeological Record* (Cambridge Univ. Press, 2010).
65. Berna, F. et al. Sediments exposed to high temperatures: reconstructing pyrotechnological processes in Late Bronze and Iron Age Strata at Tel Dor (Israel). *J. Archaeol. Sci.* **34**, 358–373 (2007).
66. Poduska, K. M. et al. Decoupling local disorder and optical effects in infrared spectra: differentiating between calcites with different origins. *Adv. Mater.* **23**, 550–554 (2011).
67. Regev, L., Poduska, K. M., Addadi, L., Weiner, S. & Boaretto, E. Distinguishing between calcites formed by different mechanisms using infrared spectrometry: archaeological applications. *J. Archaeol. Sci.* **37**, 3022–3029 (2010).
68. Marston, J. M., d'Alpoim Guedes, J. & Warinner, C. *Method and Theory in Paleoethnobotany* (Univ. Colorado Press, 2015).
69. Pearsall, D. M. *Paleoethnobotany: A Handbook of Procedures* (Routledge, 2016).
70. Kromer, B., Lindauer, S., Synal, H.-A. & Wacker, L. MAMS—a new AMS facility at the Curt-Engelhorn-Centre for Achaeometry, Mannheim, Germany. *Nucl. Instrum. Methods Phys. Res. B* **294**, 11–13 (2013).
71. Lindauer, S. et al. The local marine reservoir effect at Kalba (UAE) between the Neolithic and Bronze Age: an indicator of sea level and climate changes. *Quat. Geochronol.* **42**, 105–116 (2017).
72. Bronk Ramsey, C. Dealing with outliers and offsets in radiocarbon dating. *Radiocarbon* **51**, 1023–1045 (2009).
73. Schmid, E. *Atlas of Animal Bones* (Elsevier, 1972).
74. Pales, L. & Lambert, C. *Atlas Osteologique pour Servir a l'Identification des Mammiferes du Quaternaire* (Centre National de la Recherche Scientifique, 1971).
75. Lister, A. M. The morphological distinction between bones and teeth of fallow deer (*Dama dama*) and red deer (*Cervus elaphus*). *Int. J. Osteoarchaeol.* **6**, 119–143 (1996).
76. Zeder, M. A. & Lapham, H. A. Assessing the reliability of criteria used to identify postcranial bones in sheep, *Ovis*, and goats, *Capra*. *J. Archaeol. Sci.* **37**, 2887–2905 (2010).
77. Shipman, P., Foster, G. & Schoeninger, M. Burnt bones and teeth: an experimental study of color, morphology, crystal structure and shrinkage. *J. Archaeol. Sci.* **11**, 307–325 (1984).
78. Villa, P. & Mahieu, E. Breakage patterns of human long bones. *J. Hum. Evol.* **21**, 27–48 (1991).
79. Dominguez-Rodrigo, M., de Juana, S., Galán, A. B. & Rodríguez, M. A new protocol to differentiate trampling marks from butchery cut marks. *J. Archaeol. Sci.* **36**, 2643–2654 (2009).
80. Fernandez-Jalvo, Y. & Andrews, P. *Atlas of Taphonomic Identifications* (Springer, 2016).
81. Lyman, R. L. *Quantitative Paleozoology* (Cambridge Univ. Press, 2008).
82. Sponheimer, M. et al. Hominins, sedges, and termites: new carbon isotope data from the Sterkfontein valley and Kruger National Park. *J. Hum. Evol.* **48**, 301–312 (2005).
83. Lee-Thorp, J. et al. Isotopic evidence for an early shift to C_4 resources by Pliocene hominins in Chad. *Proc. Natl. Acad. Sci. USA* **109**, 20369–20372 (2012).
84. Carleton, C. [wccarleton/mesoneomalta: Revision 1](https://doi.org/10.5281/zenodo.14192393). Zenodo <https://doi.org/10.5281/zenodo.14192393> (2024).

Acknowledgements This article is dedicated to the memory of Christopher Foyle, who did so much to encourage, support and drive investigations into Maltese prehistory. Without him, this project would never have happened. This research was performed with the permission (SCH332/19) of the Superintendence of Cultural Heritage (Malta) and the Environment Resources Authority (EP01281/23). We are grateful to K. Farrugia and K. Borda for their support over the years. We thank Heritage Malta, in particular S. Sultana, for assistance and support in this work; the students who assisted in excavation and flotation; B. Restall for advice regarding fresh water sources; H. Russ for assistance identifying grouper remains; and S. O'Reilly and H. Sell for assistance with the main-text figures. This research was funded by the Foyle Research Institute UK (to E.M.L.S.), the European Research Council 'IslandLab' project grant no. 101041480 (E.M.L.S.), the Max Planck Society 'Lise Meitner' Excellence Scheme (E.M.L.S.), the University of Malta Research Excellence Award grant 202103 (N.C.V., R.G. and E.M.L.S.), the Generalitat de Catalunya grant SGR2021-01237 (E.A.), the Spanish Ministry of Science and Innovation 'María de Maeztu' program for Units of Excellence in R&D grant CEX2019-000945-M (E.A.) and Marie Skłodowska-Curie Actions HORIZON-MSCA-2021-PF-01 ID: 101063904 (A.B.-C.).

Author contributions Conceptualization: E.M.L.S. Project methodology: E.M.L.S., J.B., H.S.G., N.C.V. and M.S. Investigation: all authors contributed in the field or in the laboratory. Funding acquisition: E.M.L.S., N.C.V. and R.G. Project administration: E.M.L.S. and N.C.V. Supervision: J.B. and N.C.V. Writing (original draft): E.M.L.S., J.B., H.S.G., M.S., A.C., E.A., A.B.-C., S.L., W.C.C., N.C.V., K.B., R.S., P.R. and I.C. Writing (review and editing): E.M.L.S., J.B., M.S., H.S.G., I.C., E.A., A.B.-C., A.C., W.C.C., S.L., R.S., K.B., G.A., M.C., R.G., A.H., J.K., A.M., M.M.-G., N.M., K.N., P.R., J.d.G., R.X. and N.C.V.

Funding Open access funding provided by Max Planck Society.

Competing interests The authors declare no competing interests.

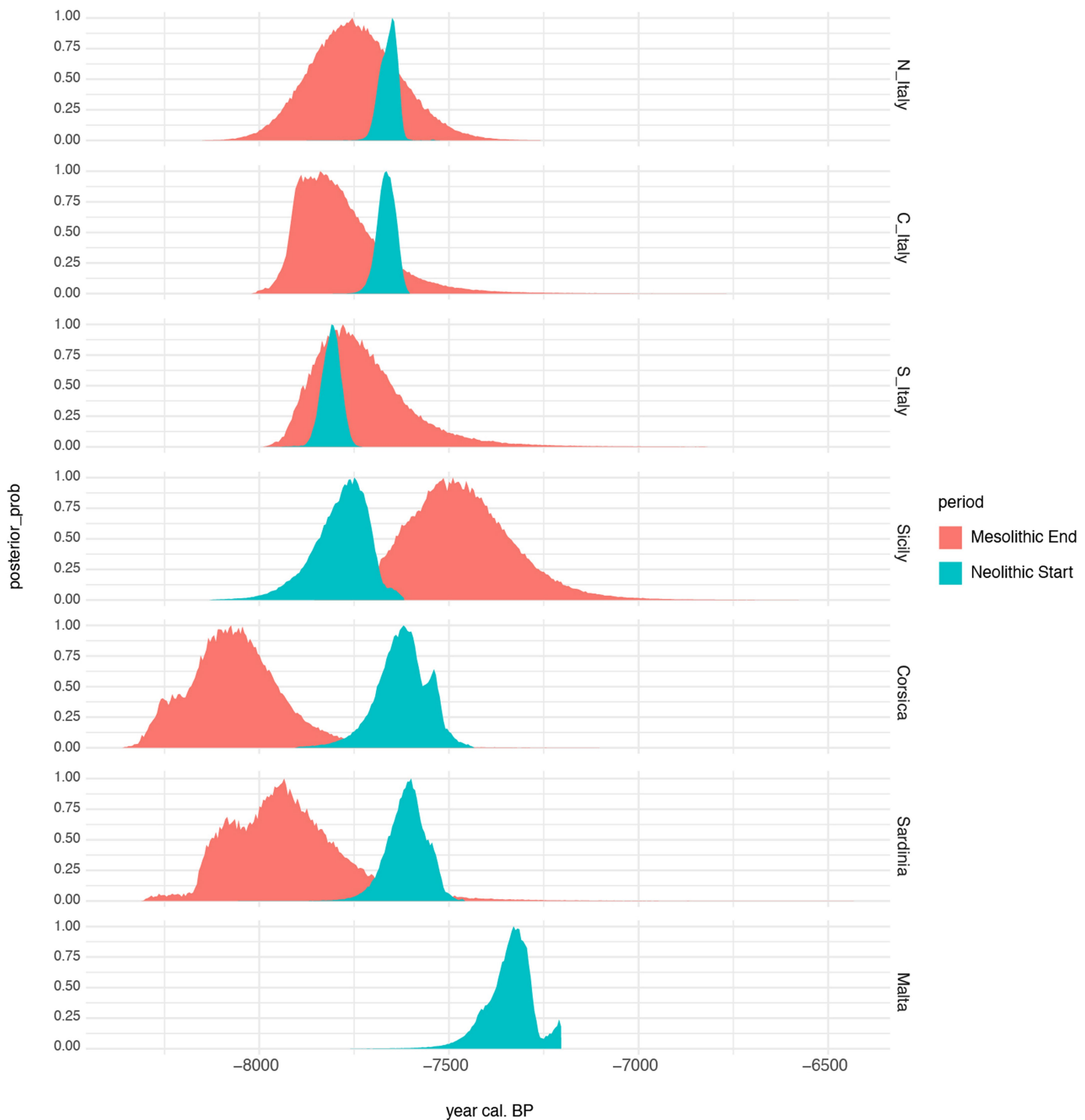
Additional information

Supplementary information The online version contains supplementary material available at <https://doi.org/10.1038/s41586-025-08780-y>.

Correspondence and requests for materials should be addressed to Eleanor M. L. Scerri, James Blinkhorn or Nicholas C. Vella.

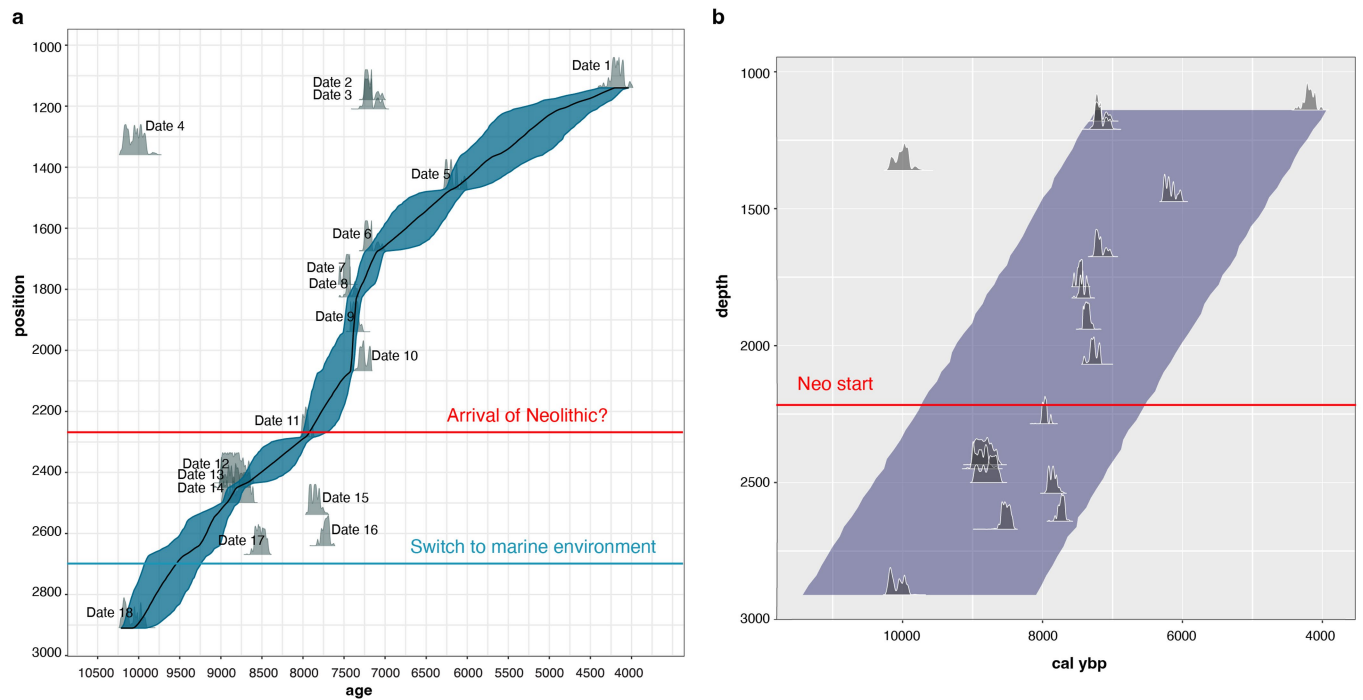
Peer review information *Nature* thanks Cyprian Broodbank, Dylan Gaffney, Carlos Duarte Simões, Sahra Talamo and the other, anonymous, reviewer(s) for their contribution to the peer review of this work.

Reprints and permissions information is available at <http://www.nature.com/reprints>.



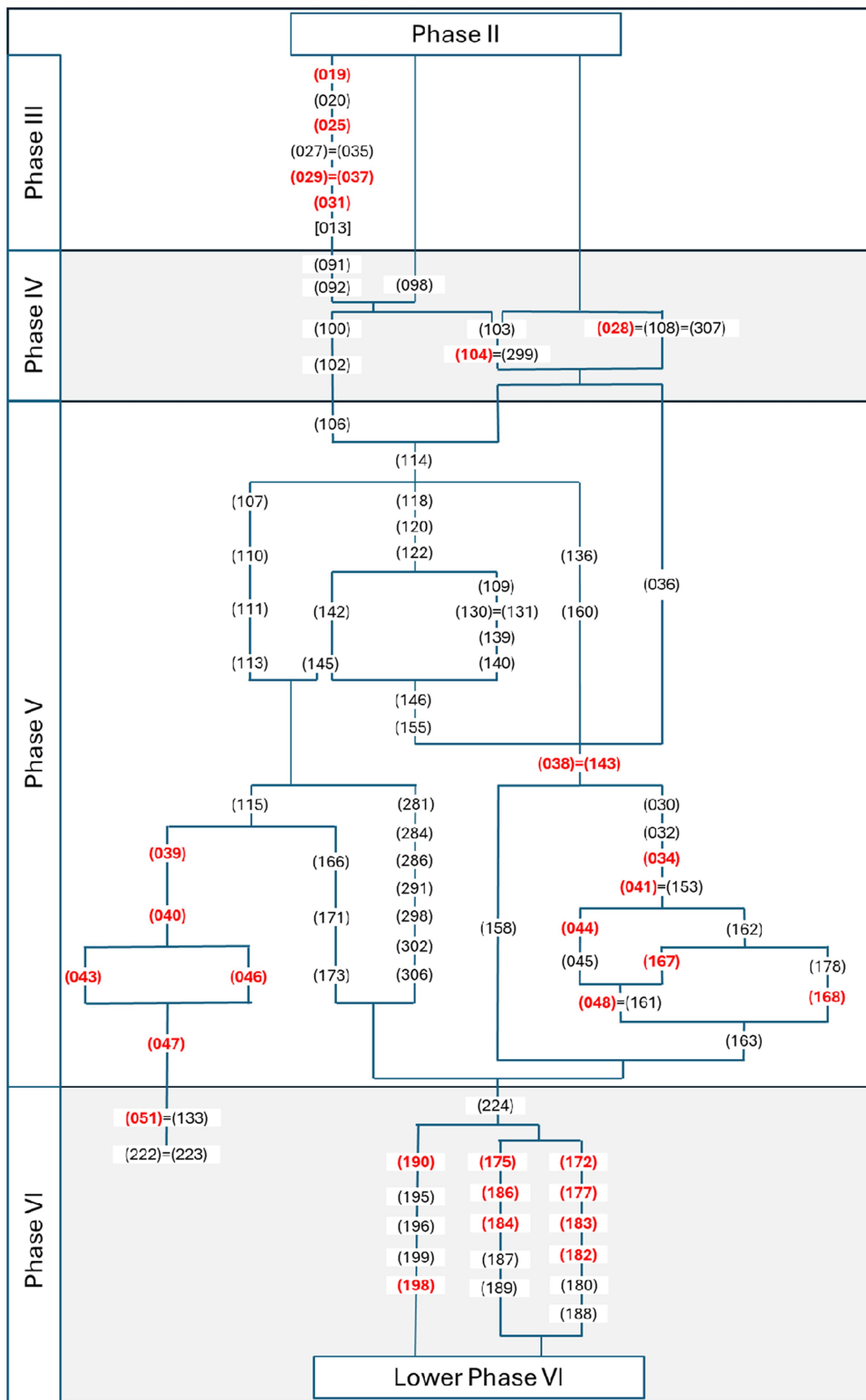
Extended Data Fig. 1 | Regional OxCal phase model of the Mesolithic-to-Neolithic transition. OxCal phase modelling of the estimated start and end dates for the Mesolithic and Neolithic phases in and around Malta¹²⁵ using the IntCal20 terrestrial calibration curve⁵⁵. Results indicate a general geographical

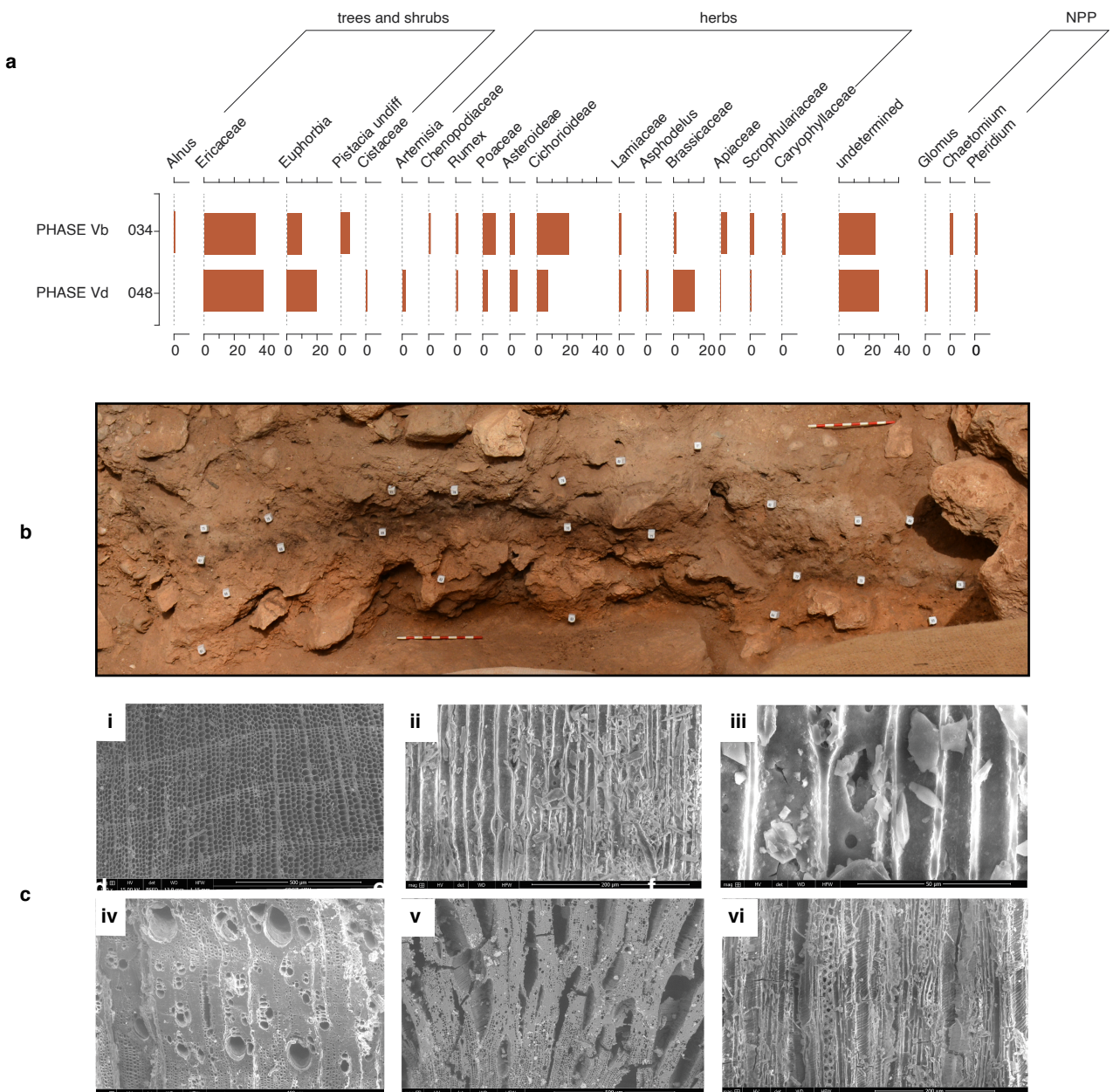
cline in the spread of the Neolithic in mainland Italy from north to south, to Sicily, Sardinia, and Corsica, and then finally to Malta. See the OxCal script in <https://github.com/wccarleton/mesoneomalta> for specifics.



Extended Data Fig. 2 | Bayesian evaluation of the earliest Maltese Neolithic. **a**, Plotted radiocarbon dates available for the sequence from the Salina Deep record in Malta, along with the pollen sequence reported by Farrell and colleagues⁴⁸, using the Bchron R package⁵², one of the methods used by Hunt and colleagues⁴⁷. Results show many potentially intrusive samples used to date

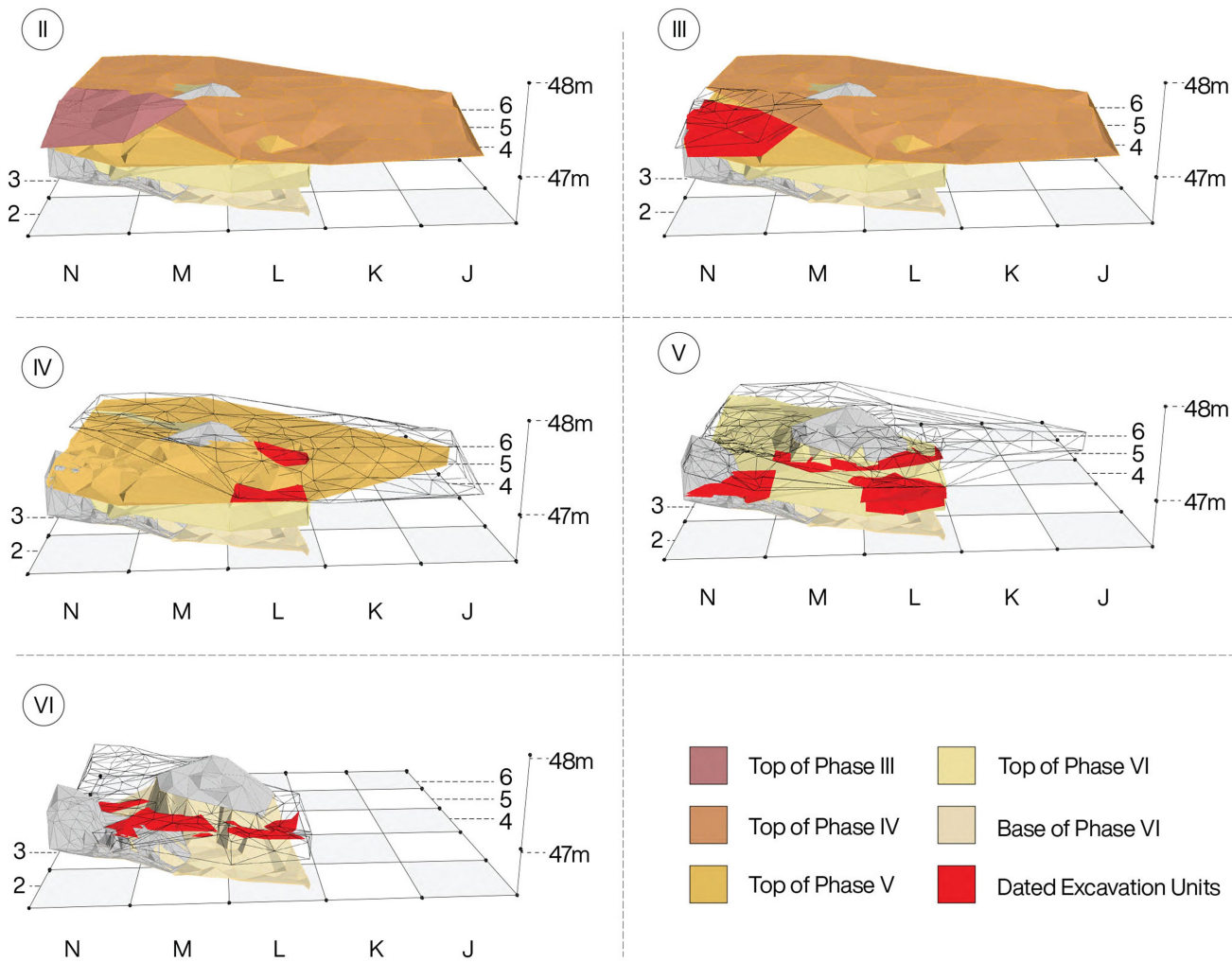
the sediments and very few sequences of dates in strict stratigraphic order. **b**, Our Bayesian regression model to relate depth to age in the Salina Deep core using the IntCal20 calibration curve⁵⁵ to calibrate the dates. The results suggest that the first Neolithic evidence in the Salina Deep record has a date with a broad error range of around two thousand years. Depth shown = cm.





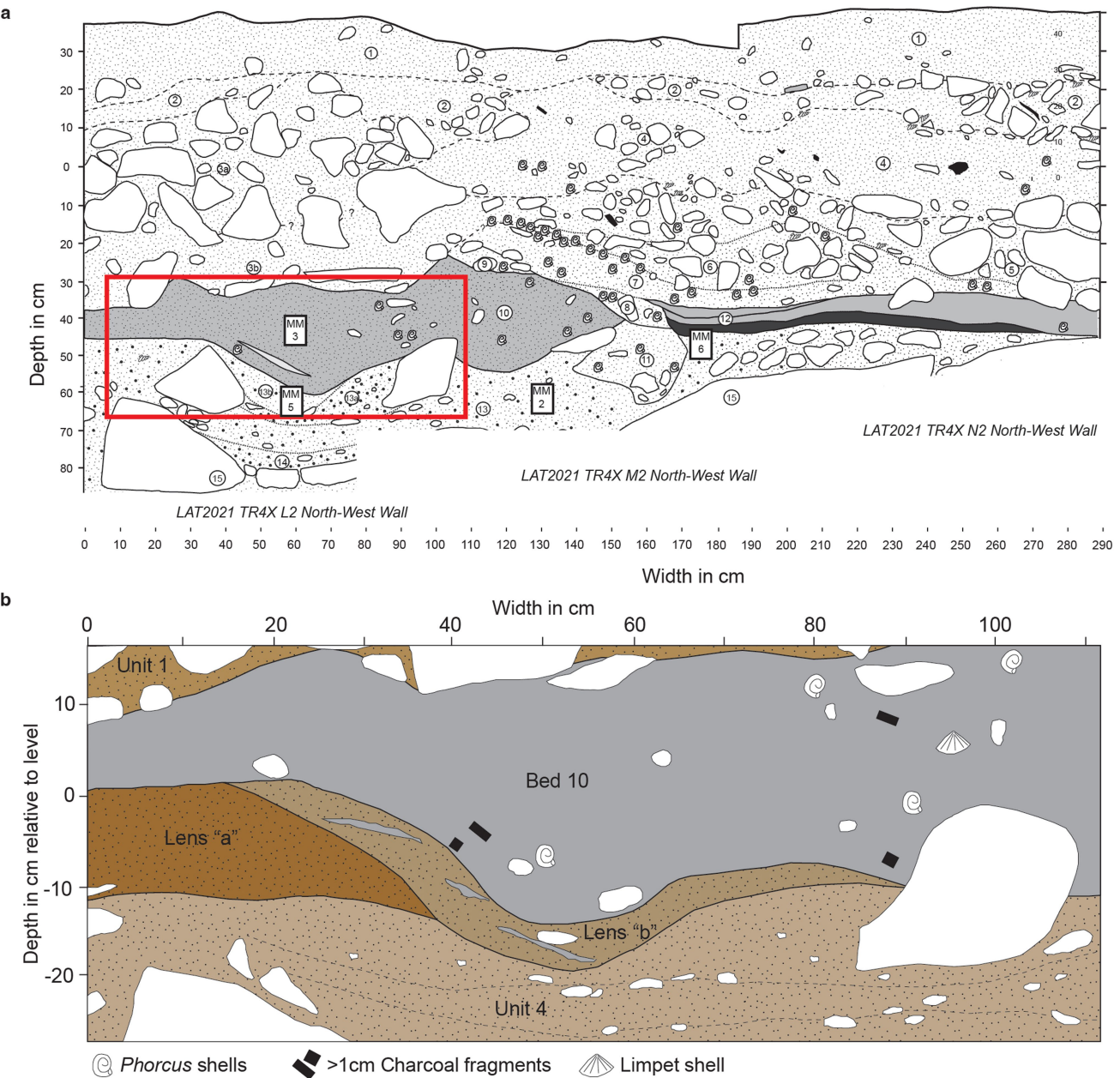
Extended Data Fig. 4 | Results of archaeobotanical analyses. **a**, Pollen diagram from Latnija archaeological site, with percentage values of pollen remains identified from contexts (034) and (048). **b**, The deep Mesolithic hearth from Phase V, square N2, with sample locations for phytolith and FTIR studies. The internal structure of the hearth can be observed, from top to bottom, combustion residue, thermal impact and natural substrate (control). **c**, ESEM images of *Pistacia cf. lentiscus* and *Juniperus* sp. charcoal remains showing wood anatomical characters: (i) *Juniperus* sp. charcoal fragment

tangential section; (ii) *Juniperus* sp. charcoal fragment tangential section showing rays and tracheids; (iii) *Juniperus* sp. charcoal fragment tangential section showing a detail of tracheid pits; (iv) *Pistacia cf. lentiscus* charcoal fragment transverse section showing ring porous distribution and vessel clusters; (v) *Pistacia cf. lentiscus* charcoal fragment tangential section showing spiral thickenings and biseriated rays; (vi) *Pistacia* sp. charcoal fragment transverse section showing cracks and vitrification altering the wood cell structure.



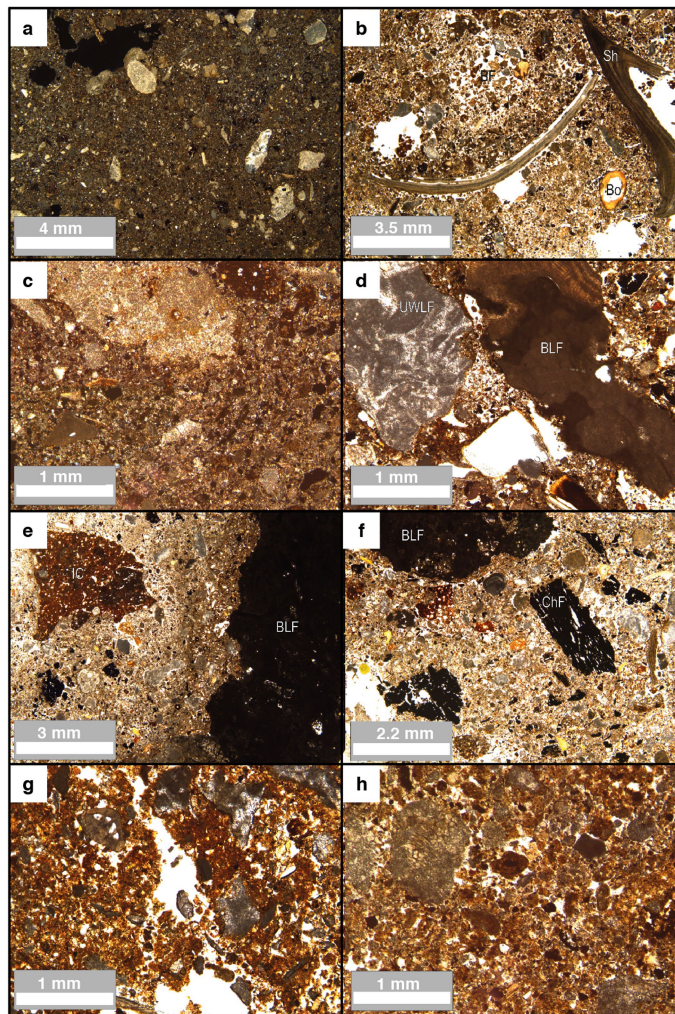
Extended Data Fig. 5 | Chronological sample locations. Oblique view illustrating the location of dated contexts (red) with respect to sediment phase boundaries spanning grid squares J–N, showing the distribution of sediments at the base of Phase II; the location of dated contexts from Phase III, with the upper boundary of Phase III deposits shown as a wireframe; the location of

dated contexts from Phase IV, with the upper boundary of Phase IV deposits shown as a wireframe; the location of dated contexts from Phase V, with the upper boundary of Phase V deposits shown as a wireframe; and the location of dated contexts from Phase VI, with the upper boundary of Phase VI deposits shown as a wireframe.

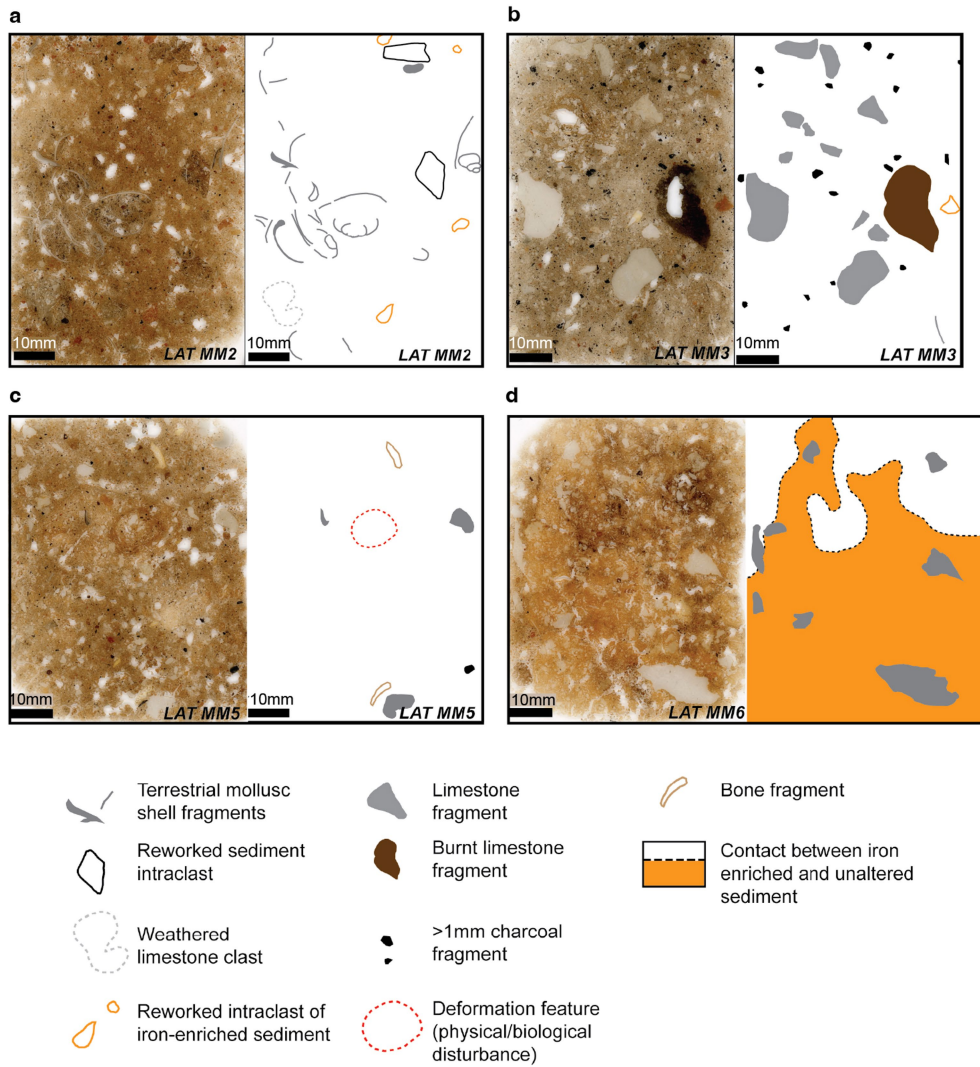


Extended Data Fig. 6 | Section drawing. **a**, Section drawing of the Latnija exposure with the detailed section shown in Fig. 3 highlighted (recorded September 2022). **b**, Detailed record of the contact between the upper part of Unit 4 and the lower contact of Bed 10 (for location of the recorded section

see Fig. 1). The section was recorded in September 2024, note that some of the large clasts that were recorded in the September 2022 section (a) had been removed from the section by September 2024.

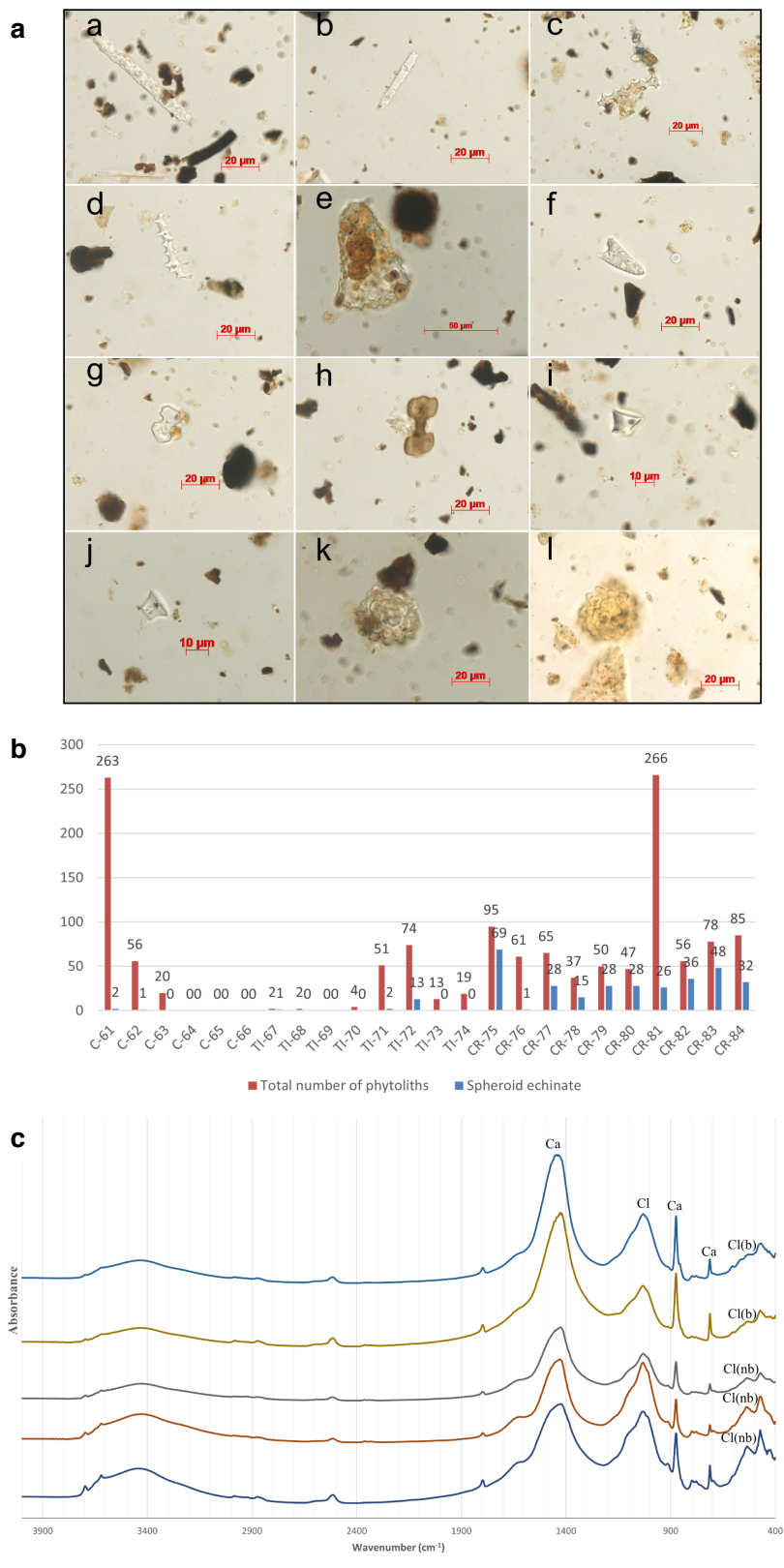

Extended Data Fig. 7 | Photomicrographs of the Latnija sediments.

a, Overview of the sediments of Unit 1. The sediments are dominated by limestone derived clasts and fine-grained material. The clear grains are fine-sand/silt sized grains of quartz. **b**, Biological material within Unit 1 (Sh – shell, Bo – Bone, BF – Burrow fill). **c**, Overview of the sediments of Unit 2 (Bed 10). The high birefringence colours show the dominance of limestone material in both the coarse and fine component. **d**, Limestone clasts within Bed 10 showing unweathered limestone fragments (UWLF) and blackened, burnt limestone fragments (BLF). **e**, Burnt limestone fragment (BLF) next to an iron oxide enriched intraclast (IC) of reworked sediment. **f**, Charcoal Fragment (ChF) and Burnt limestone fragment (BLF) in Bed 10. **g**, Iron enriched sediments of Unit 1 from directly below the contact with Bed 12. **h**, Pelleted microfabric of lens b below Bed 10.



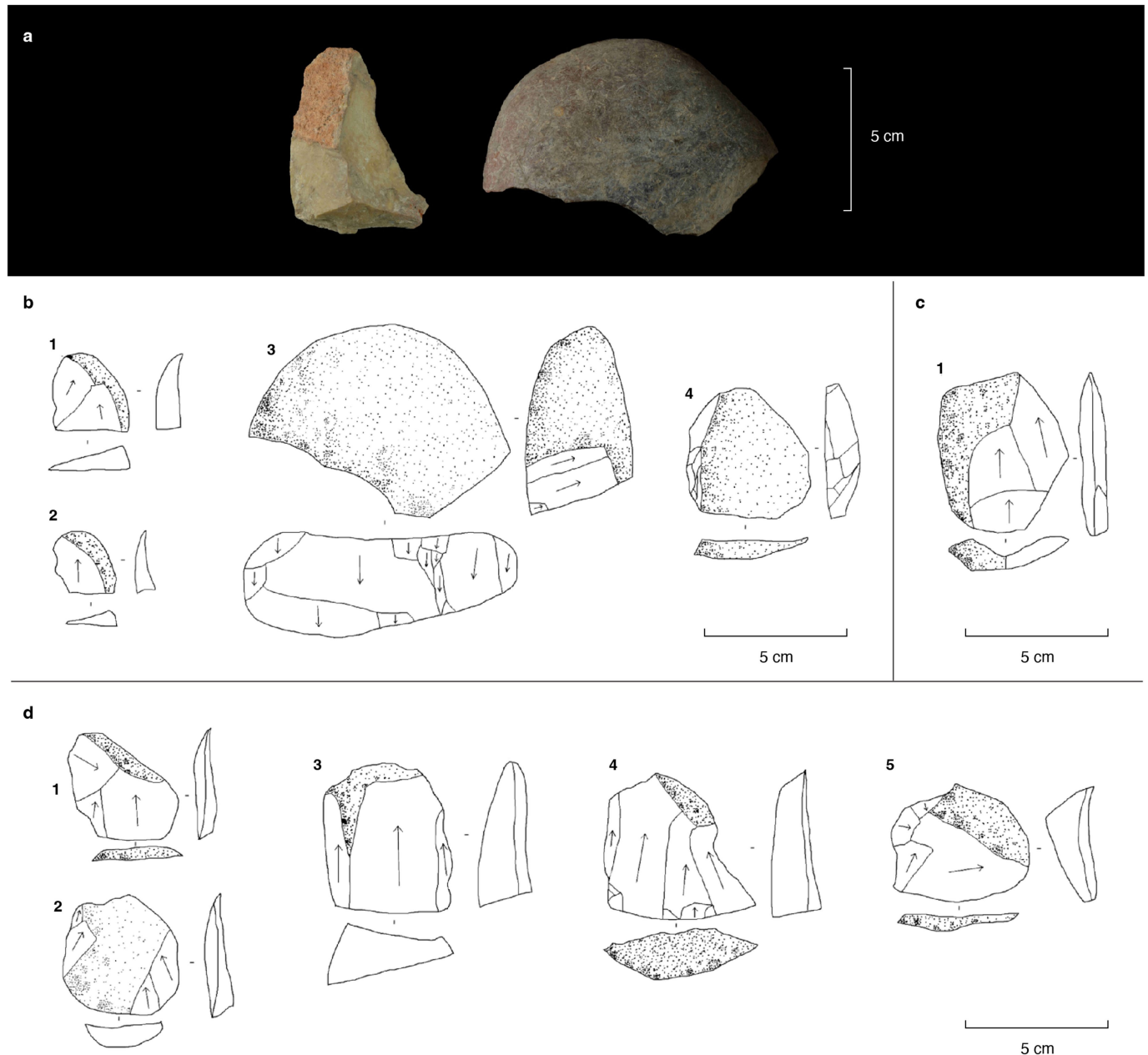
Extended Data Fig. 8 | High-resolution scans of micromorphological thin sections from the Latnija sequence. See Extended Data Fig. 6 and sediment section (Supplementary Information 2) for the location of thin-section samples. **a**, MM2 is taken from the unaltered sediments at the base of the sequence. This sample presents the key characteristics of patterns of sedimentation prior to the Mesolithic occupation. These can be summarized as consisting of: 1) rare limestone clasts (frequently showing evidence for in situ decay), 2) intraclasts of reworked sediment and 3) fragments of terrestrial mollusc shell. Limited materials that are indicative of burning or burning products are present. **b**, MM3 is taken from the ash-rich sediments of the sequence, a factor that can be seen in the colour difference between the brown matrix of MM2 and the grey matrix of MM3. MM3 is rich in >1 mm sized charcoal fragments and limestone clasts, some of which show evidence for a strong degree of burning. **c**, MM5 is taken from the

contact between the ash-rich sediment (MM3) and the underlying cave floor sediment (MM2). The sediment of MM5 is, consequently, characterized by a mixture of both sediment types. Charcoal fragments are abundant (but only rarely >1 mm) but the matrix overall is more typical of MM2. Bone fragments are present as are circular features that are characteristics of deformation which could be either biological or physical in origin. The sediments have formed in association with cutting into pre-existing sediments prior to the deposition of the ash-rich sediments. **d**, MM6 is taken from below darkened sediment believed to be in situ burning. The sediments of MM6 are more reddened than any other sampled sediments and occur directly below sediments the colour of which are more typical of the unaltered cave sediments of MM2. This unit is interpreted as being thermally altered as a direct result of in situ burning directly above these deposits.



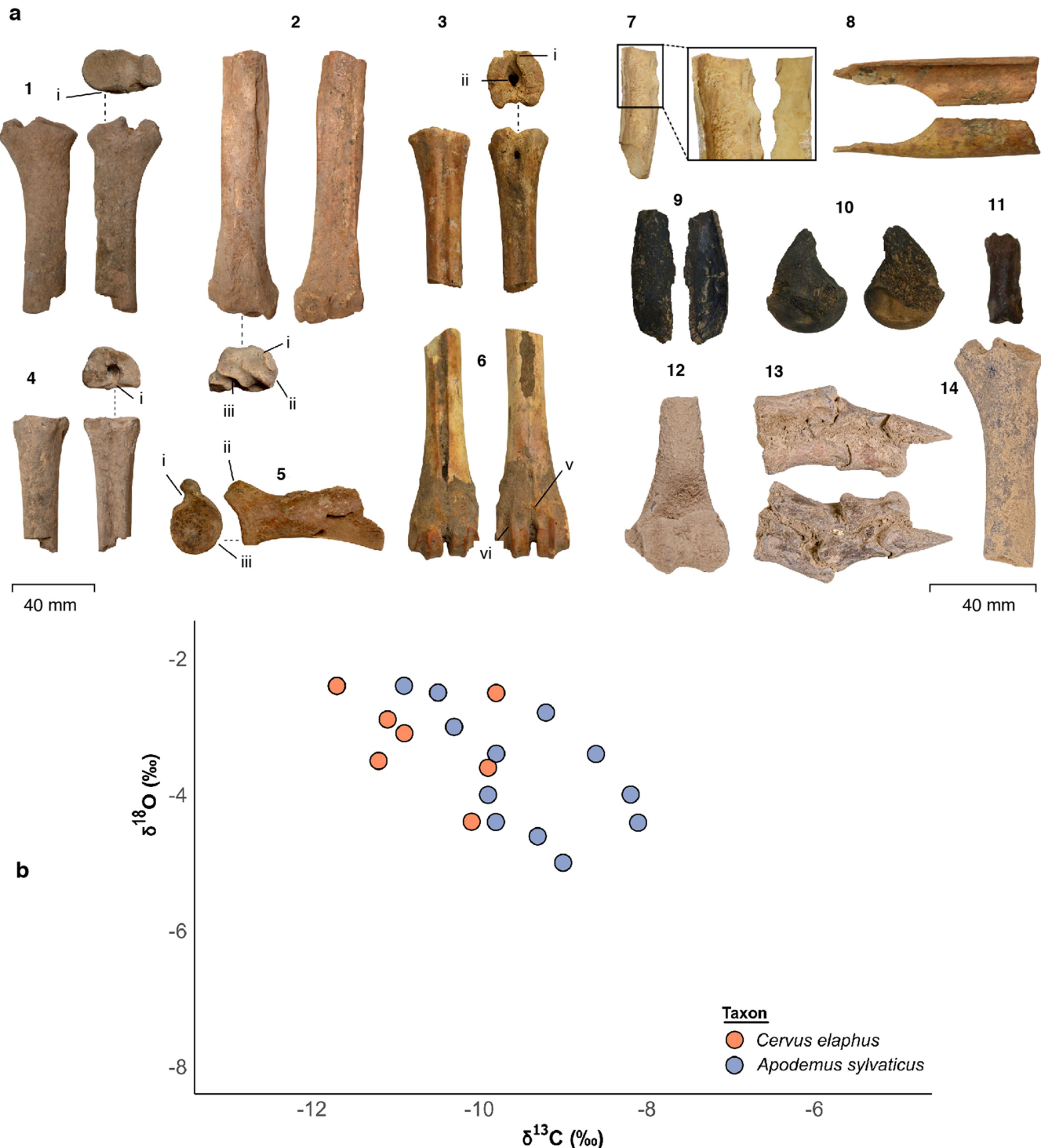
Extended Data Fig. 9 | Phytolith study. **a**, Phytoliths image identified in the Phase V deep hearth. **a,b**, Elongate entire from grass leaf; **c,d**, Elongate dentate from grass inflorescence; **e**, Bulliform flabellate from grass leaf; **f**, Acute bulbous from grasses leaf; **g,h**, GSSCP Bilobate from grasses-C4; **i-j**, GSSCP Rondel from grasses-C3; **k,l**, Spheroid echinate from Palms. **b**, Different dynamics of phytoliths identified in the layers that make up the hearth in

relation to the number of phytoliths identified as spheroid echinate in each sample. Key: C, Control; TI, Thermal Impact; CR, Combustion Residue. **c**, Infrared spectra of sediments from some representative samples. Key: C, Control; TI, Thermal Impact; CR, Combustion Residue; Ca, Calcite; Cl, Clay; Qz, quartz; b, thermally altered clay; nb, not thermally altered clay.



Extended Data Fig. 10 | Lithics from the Maltese Mesolithic. **a**, Photographs of lithics from Phase III (left) and Phase V (right) showing terrestrial and coastal raw material forms. **b-d**, Illustrations of lithics from Phases V (**b**), IV (**c**) and III (**d**). All are flakes except b3 (core) and b4 (retouched flake). All limestone.

Article



Extended Data Fig. 11 | Taxonomic and isotopic analyses of faunal remains.

Red deer remains, taphonomic modifications, and stable isotope results.

a, Remains of red deer including a proximal radius (1), distal radius (b), proximal metatarsal (3), proximal metacarpal (4), scapula (5), and a distal metatarsal (6). Examples of taphonomic modifications including a midshaft fragment with a

green fracture and a double notch with corresponding negative flake scars (7), a midshaft fragment with a green fracture (8), examples of charred bone (9–11), and examples of bone covered in adhering matrix (12–14). **b**, Results of the stable carbon $\delta^{13}\text{C}$ and $\delta^{18}\text{O}$ analysis by taxa. Roman numerals refer to ref. 75. Left scale bar applies to A1–6 and right scale bar to A7–14.

Reporting Summary

Nature Portfolio wishes to improve the reproducibility of the work that we publish. This form provides structure for consistency and transparency in reporting. For further information on Nature Portfolio policies, see our [Editorial Policies](#) and the [Editorial Policy Checklist](#).

Statistics

For all statistical analyses, confirm that the following items are present in the figure legend, table legend, main text, or Methods section.

n/a Confirmed

- The exact sample size (n) for each experimental group/condition, given as a discrete number and unit of measurement
- A statement on whether measurements were taken from distinct samples or whether the same sample was measured repeatedly
- The statistical test(s) used AND whether they are one- or two-sided
 - Only common tests should be described solely by name; describe more complex techniques in the Methods section.*
- A description of all covariates tested
- A description of any assumptions or corrections, such as tests of normality and adjustment for multiple comparisons
- A full description of the statistical parameters including central tendency (e.g. means) or other basic estimates (e.g. regression coefficient) AND variation (e.g. standard deviation) or associated estimates of uncertainty (e.g. confidence intervals)
- For null hypothesis testing, the test statistic (e.g. F , t , r) with confidence intervals, effect sizes, degrees of freedom and P value noted
 - Give P values as exact values whenever suitable.*
- For Bayesian analysis, information on the choice of priors and Markov chain Monte Carlo settings
- For hierarchical and complex designs, identification of the appropriate level for tests and full reporting of outcomes
- Estimates of effect sizes (e.g. Cohen's d , Pearson's r), indicating how they were calculated

Our web collection on [statistics for biologists](#) contains articles on many of the points above.

Software and code

Policy information about [availability of computer code](#)

Data collection

Data analysis https://github.com/wccarleton/mesoneomalta"/>

For manuscripts utilizing custom algorithms or software that are central to the research but not yet described in published literature, software must be made available to editors and reviewers. We strongly encourage code deposition in a community repository (e.g. GitHub). See the Nature Portfolio [guidelines for submitting code & software](#) for further information.

Data

Policy information about [availability of data](#)

All manuscripts must include a [data availability statement](#). This statement should provide the following information, where applicable:

- Accession codes, unique identifiers, or web links for publicly available datasets
- A description of any restrictions on data availability
- For clinical datasets or third party data, please ensure that the statement adheres to our [policy](#)

Code and Data are available: <https://github.com/wccarleton/mesoneomalta> , and archived <https://doi.org/10.5281/zenodo.14192393>

Research involving human participants, their data, or biological material

Policy information about studies with [human participants or human data](#). See also policy information about [sex, gender \(identity/presentation\), and sexual orientation](#) and [race, ethnicity and racism](#).

Reporting on sex and gender	<input type="checkbox"/> There were no human participants or human biological material used in this paper.
Reporting on race, ethnicity, or other socially relevant groupings	n/a
Population characteristics	n/a
Recruitment	n/a
Ethics oversight	n/a

Note that full information on the approval of the study protocol must also be provided in the manuscript.

Field-specific reporting

Please select the one below that is the best fit for your research. If you are not sure, read the appropriate sections before making your selection.

Life sciences Behavioural & social sciences Ecological, evolutionary & environmental sciences

For a reference copy of the document with all sections, see nature.com/documents/nr-reporting-summary-flat.pdf

Ecological, evolutionary & environmental sciences study design

All studies must disclose on these points even when the disclosure is negative.

Study description	The study involved archaeological investigations of the material culture traces of past humans.
Research sample	100% sampling of sediments was undertaken to recover archaeobotanical remains (phytoliths, anthracology, pollen). All material culture and faunal remains were collected and recorded using a Total Station where they measured over 2mm, with the exception of microfaunal remains. Charcoal was recovered from the sediments and large pieces collected in situ and recorded using a total station for chronometric dating.
Sampling strategy	Archaeobotanical analyses involved 100% sampling and all sediments were floated and analysed. Charcoal for chronometric dating was selected from key contexts using the Harris Matrix and features such as hearths to make decisions on Phase boundaries and the remains of human activity.
Data collection	Data was collected during excavation. Context sheets, photographs, photogrammetry and total station recording as well as plan drawings were used to ensure detailed and correct documentation. All samples, artefacts and bones were also recorded using a total station in order to reconstruct their location in three dimensions.
Timing and spatial scale	Data was collected during three field seasons. Field seasons in 2021 (4 weeks), 2022 (4 weeks) and 2023 (4 weeks) provided the data reported in the paper. The Data was recovered from a 5 x 5 m trench.
Data exclusions	No data was excluded.
Reproducibility	We provide tables of raw data and analytical code, as well as abundant details on the location and character of scientific samples that ensure reproducibility.
Randomization	This is not relevant to an archaeological study reporting the results of an excavation.
Blinding	For the reasons described above, this is not relevant.

Did the study involve field work? Yes No

Field work, collection and transport

Field conditions	The fieldwork was conducted in the summer months of August and September which was mostly warm and dry with the exception of some storm events. Thanks to preparation involving sand bags and rainproof covers, these storms did not impact the excavations.
Location	Mellieha, Malta 35.977703617820254, 14.328625741239756

Access & import/export

All excavation work was conducted under permits provided by the Maltese Superintendence of Cultural Heritage and the Environmental Resource Agency. Individual samples exported for analyses were given individual permissions for export and analysis by the Superintendence of Cultural Heritage.

Disturbance

The area of the trench has been disturbed by excavation, but the trench is backfilled every year and there is no impact on the broader location of the trench.

Reporting for specific materials, systems and methods

We require information from authors about some types of materials, experimental systems and methods used in many studies. Here, indicate whether each material, system or method listed is relevant to your study. If you are not sure if a list item applies to your research, read the appropriate section before selecting a response.

Materials & experimental systems

n/a	Involved in the study
<input checked="" type="checkbox"/>	Antibodies
<input checked="" type="checkbox"/>	Eukaryotic cell lines
<input type="checkbox"/>	Palaeontology and archaeology
<input checked="" type="checkbox"/>	Animals and other organisms
<input checked="" type="checkbox"/>	Clinical data
<input checked="" type="checkbox"/>	Dual use research of concern
<input type="checkbox"/>	Plants

Methods

n/a	Involved in the study
<input checked="" type="checkbox"/>	ChIP-seq
<input checked="" type="checkbox"/>	Flow cytometry
<input checked="" type="checkbox"/>	MRI-based neuroimaging

Palaeontology and Archaeology

Specimen provenance

Faunal remains were recovered from the site. Most of the analyses on the faunal remains have taken place in Malta under the excavation permit. All faunal remains that have been exported for specific analyses have the permission of the Superintendence of Cultural Heritage on an individual basis.

Specimen deposition

Currently the specimens are being held at the University of Malta. They will be given to Heritage Malta for accessioning and long term storage once the project is completed.

Dating methods

Radiocarbon dating was used on charcoal. One date was obtained on bone. Permission for the expert of both bone and charcoal was sought and received from the Superintendence of Cultural Heritage. ABA Pre-treatment was used at the CEZA institute in Mannheim Germany, for the charcoal remains. The bone date was obtained from the Center for Applied Isotope Studies (CAIS) in the U.S. Details of treatments are given in the methods section of the main text.

Tick this box to confirm that the raw and calibrated dates are available in the paper or in Supplementary Information.

Ethics oversight

No ethical approval or guidance was required for the dating of charcoal and faunal remains.

Note that full information on the approval of the study protocol must also be provided in the manuscript.

Dual use research of concern

Policy information about [dual use research of concern](#)

Hazards

Could the accidental, deliberate or reckless misuse of agents or technologies generated in the work, or the application of information presented in the manuscript, pose a threat to:

No	Yes
<input checked="" type="checkbox"/>	Public health
<input checked="" type="checkbox"/>	National security
<input checked="" type="checkbox"/>	Crops and/or livestock
<input checked="" type="checkbox"/>	Ecosystems
<input checked="" type="checkbox"/>	Any other significant area

Experiments of concern

Does the work involve any of these experiments of concern:

No	Yes
<input checked="" type="checkbox"/>	Demonstrate how to render a vaccine ineffective
<input checked="" type="checkbox"/>	Confer resistance to therapeutically useful antibiotics or antiviral agents
<input checked="" type="checkbox"/>	Enhance the virulence of a pathogen or render a nonpathogen virulent
<input checked="" type="checkbox"/>	Increase transmissibility of a pathogen
<input checked="" type="checkbox"/>	Alter the host range of a pathogen
<input checked="" type="checkbox"/>	Enable evasion of diagnostic/detection modalities
<input checked="" type="checkbox"/>	Enable the weaponization of a biological agent or toxin
<input checked="" type="checkbox"/>	Any other potentially harmful combination of experiments and agents

Plants

Seed stocks

No seed stocks were used. We looked at burned and mineralized plant remains as well as pollen.

Novel plant genotypes

N/a

Authentication

N/a